

# CHAPTER 1

## Measuring the Muon Neutrino Magnetic Moment

TO DO: *Also check out NeutrinoMassesPheno2007.pdf, sec 6.4*

TO DO: *Write an introduction to the NuMM*

### 1.1 Theory of neutrino magnetic moment

As was describe in Sec. ??, neutrinos in the Standard Model (SM) are massless and electrically neutral particles. However, even SM neutrinos can have electromagnetic interaction through loop diagrams involving charged leptons and the W boson. These interactions are described by the neutrino charge radius, described in section 1.1.2 TO DO: *Re-write this since I'm not going to include the other elmag properties section [1]*.

In general Beyond Standard Model (BSM) theories, considering interactions with a single photon as shown on Fig. 1.1, neutrino electromagnetic interactions can be described by an *effective* interaction Hamiltonian [2]

$$\mathcal{H}_{em}^{(\nu)}(x) = \sum_{k,j=1}^N \bar{\nu}_k(x) \Lambda_\mu^{kj} \nu_j(x) A^\mu(x). \quad (1.1)$$

Here  $\nu_k(x)$ ,  $k = 1, \dots, N$ , are neutrino fields in the mass basis with  $N$  neutrino mass states and  $x$  denotes the position.  $\Lambda_\mu^{kj}$  is a general vertex function and  $A^\mu(x)$  is the electromagnetic field.

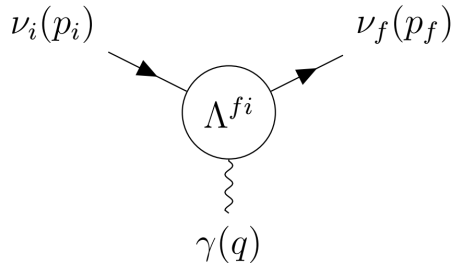


Figure 1.1: Effective coupling of neutrinos with one photon electromagnetic field.

The vertex function  $\Lambda_\mu^{fi}(q)$  is generally a matrix and in the most general case consistent with the **SM** gauge invariance [3, 4] can be written in terms of linearly independent products of Dirac matrices ( $\gamma$ ) and only depends on the four momentum of the photon ( $q = p_f - p_i$ ):

$$\begin{aligned}\Lambda_\mu^{fi}(q) = & \mathbb{F}_1^{fi}(q^2) q_\mu + \mathbb{F}_2^{fi}(q^2) q_\mu \gamma_5 + \mathbb{F}_3^{fi}(q^2) \gamma_\mu + \mathbb{F}_4^{fi}(q^2) \gamma_\mu \gamma_5 + \\ & \mathbb{F}_5^{fi}(q^2) \sigma_{\mu\nu} q^\nu + \mathbb{F}_6^{fi}(q^2) \epsilon_{\mu\nu\rho\gamma} q^\nu \sigma^{\rho\gamma},\end{aligned}\quad (1.2)$$

where  $\mathbb{F}_i^{fi}(q^2)$  are six Lorentz invariant form factors and  $\delta$  and  $\epsilon$  are the Dirac delta and the Levi-Civita symbols respectively.

Applying conditions of hermiticity ( $\mathcal{H}_{em}^{(\nu)\dagger} = \mathcal{H}_{em}^{(\nu)}$ ) and of the gauge invariance of the electromagnetic field, the vertex function can be rewritten as

$$\Lambda_\mu^{fi}(q) = (\gamma_\mu - q_\mu \not{q}/q^2) \left[ \mathbb{F}_Q^{fi}(q^2) + \mathbb{F}_A^{fi}(q^2) q^2 \gamma_5 \right] - i \sigma_{\mu\nu} q^\nu \left[ \mathbb{F}_M^{fi}(q^2) + i \mathbb{F}_E^{fi}(q^2) \gamma_5 \right], \quad (1.3)$$

where  $\mathbb{F}_Q^{fi}$ ,  $\mathbb{F}_M^{fi}$ ,  $\mathbb{F}_E^{fi}$  and  $\mathbb{F}_A^{fi}$  are hermitian matrices representing the charge, dipole magnetic, dipole electric and anapole neutrino form factors respectively. It is clear that the vertex function only depends on the square of the four momentum of the photon  $q^2$ . In coupling with a real photon ( $q^2 = 0$ ) these form factors become the neutrino charge and magnetic, electric and anapole moments. The neutrino charge radius corresponds to the second term in the expansion of the charge form factor [2].

The above expression can be simplified as [5]

$$\Lambda_\mu^{fi}(q) = \gamma_\mu \left( Q_{\nu_{fi}} + \frac{q^2}{6} \langle r^2 \rangle_{\nu_{fi}} \right) - i \sigma_{\mu\nu} q^\nu \mu_{\nu_{fi}}, \quad (1.4)$$

where  $Q_{\nu_{fi}}$ ,  $\langle r^2 \rangle_{\nu_{fi}}$ , and  $\mu_{\nu_{fi}}$  are the neutrino charge, effective charge radius (also containing anapole moment), and an effective magnetic moment (also containing electric moment) respectively. This is possible thanks to the similar effect of the neutrino charge radius and the anapole moment, or of the neutrino magnetic and electric moment respectively [2]. These are the three neutrino electromagnetic properties (charge, charge radius and magnetic moment) measured in the experiments.

**TO DO:** Add a note briefly describing the other elmag properties and mentioning that they could be measured as well, but not describe here. Maybe refer reader to the

*theoretical overview paper*

### 1.1.1 Neutrino electric and magnetic dipole moments

The size and effect of neutrino electromagnetic properties depend on the specific BSM theory. Evaluating the one loop diagrams in the minimally extended SM with three right-handed Dirac neutrinos as described in Sec. ?? gives the first approximation of the electric and magnetic moments:

$$\left. \begin{aligned} \mu_{kj}^D \\ i\epsilon_{kj}^D \end{aligned} \right\} \simeq \frac{3eG_F}{16\sqrt{2}\pi^2} (m_k \pm m_j) \left( \delta_{kj} - \frac{1}{2} \sum_{l=e,\mu,\tau} U_{lk}^\star U_{lj} \frac{m_l^2}{m_W^2} \right), \quad (1.5)$$

where  $m_k, m_j$  are the neutrino masses and  $m_l$  are the masses of charged leptons which appear in the loop diagrams [2]. Also,  $D$  superscript denotes Dirac neutrinos,  $e$  is the electron charge,  $G_F$  is the Fermi coupling constant, and  $U$  is the Pontecorvo-Maki-Nakagawa-Sakata (PMNS) neutrino oscillation matrix. Higher order electromagnetic corrections were neglected, but can also have a significant contribution, depending on the theory.

It can be seen that Dirac neutrinos have no diagonal electric moments ( $\epsilon_{kk}^D = 0$ ) and their diagonal magnetic moments are approximately

$$\mu_{kk}^D \simeq \frac{3eG_F m_k}{8\sqrt{2}\pi^2} \simeq 3.2 \times 10^{-19} \left( \frac{m_k}{\text{eV}} \right) \mu_B, \quad (1.6)$$

where  $\mu_B$  is the Bohr magneton which represents the value of the electron magnetic moment [2]. Neutrino magnetic moments are therefore strongly suppressed by the smallness of neutrino masses, with theoretical predictions in Eq. 1.6 several orders of magnitude below the reach of current experiments [5].

The transition magnetic moments from Eq. 1.5 are suppressed with respect to the largest of the diagonal magnetic moments by at least a factor of  $10^{-4}$  due to the  $m_W^2$  in the denominator. The transition electric moments are even smaller due to the mass difference in Eq. 1.5. Therefore an experimental observation of a magnetic moment larger than in Eq. 1.6 would indicate physics beyond the minimally extended SM [2, 6].

*TODO: Actually write why these values are different for Majorana neutrinos than for Dirac neutrinos* Majorana neutrinos in a minimal extension can be obtained by either

adding a  $SU(2)_L$  Higgs triplet, or right handed neutrinos together with a  $SU(2)_L$  Higgs singlet [2]. If we neglect the Feynman diagrams which depend on the model of the scalar sector, the magnetic and electric dipole moments are

$$\mu_{kj}^M \simeq -\frac{3ieG_F}{16\sqrt{2}\pi^2} (m_k + m_j) \sum_{l=e,\mu,\tau} \text{Im}[U_{lk}^\star U_{lj}] \frac{m_l^2}{m_W^2}, \quad (1.7)$$

$$\epsilon_{kj}^M \simeq \frac{3ieG_F}{16\sqrt{2}\pi^2} (m_k - m_j) \sum_{l=e,\mu,\tau} \text{Re}[U_{lk}^\star U_{lj}] \frac{m_l^2}{m_W^2}. \quad (1.8)$$

These are difficult to compare to the Dirac case, due to possible presence of Majorana phases in the PMNS matrices, but it is clear that they have the same order of magnitude as Dirac transition dipole moments. However, the neglected model dependent contributions can enhance the transition dipole moments [2].

**TO DO:** *Re-read the natural upper bounds paper* It is possible [6] to obtain a ‘natural’ upper limits on the size of the neutrino magnetic moment by calculating its contribution to the neutrino mass by standard model radiative corrections. **TO DO:** *I don’t think this is clear enough, how is this done* For Dirac neutrinos, the radiative correction induced by neutrino magnetic moment, generated at an energy scale  $\Lambda_{NP}$ , to the neutrino mass is generically

$$m_\nu^D \sim \frac{\mu_\nu^D}{3 \times 10^{-15} \mu_B} [\Lambda(\text{TeV})]^2 \text{eV}. \quad (1.9)$$

So for  $\Lambda_{NP} \simeq 1\text{TeV}$  and  $m_\nu \lesssim 0.3\text{eV}$  the limit becomes  $\mu_\nu^D \lesssim 10^{-15} \mu_B$ . This applies only if New Physics (NP) is well above the electroweak scale ( $\Lambda_{EW} \sim 100\text{GeV}$ )

**TO DO:** *Finish this sentence.* However, there are theories that contain a Dirac neutrino magnetic moment higher than this limit, for example in frameworks of minimal super-symmetric standard model, by adding more Higgs doublets, or by considering large extra dimensions **TO DO:** *Add references to the specific theories?* [2].

Similar limit for Majorana neutrino magnetic moment would be less stringent than for Dirac neutrinos due to the antisymmetry of the Majorana neutrino magnetic moment form factors **TO DO:** *Probably explain here a bit more what does this mean.*

Considering  $m_\nu \lesssim 0.3\text{eV}$ , the limit can be expressed as

$$\mu_{\tau\mu}, \mu_{\tau e} \lesssim 10^{-9} [\Lambda (\text{TeV})]^{-2} \quad (1.10)$$

$$\mu_{\mu e} \lesssim 3 \times 10^{-7} [\Lambda (\text{TeV})]^{-2} \quad (1.11)$$

which is shown in the flavour basis **TO DO: Explain here what is the flavour basis**, which relates to the framework used previously via the **PMNS** matrix as

$$\mu_{ij} = \sum_{\alpha\beta} \mu_{\alpha\beta} U_{\alpha i}^* U_{\beta j}, \quad \alpha, \beta \in \{e, \mu, \tau\}. \quad (1.12)$$

**TO DO: Add a discussion about the triangular inequalities**

These considerations imply, that if a magnetic moment  $\mu \gtrsim 10^{-15} \mu_B$  would be measured, it is more plausible that neutrinos are Majorana fermions and that the scale of lepton violation would be well below the conventional see-saw scale [6] **TO DO: double check this claim, also reword this sentence.**

### Effective neutrino magnetic moment

Since experiments detect neutrino flavour states, not the mass states, what we measure is an effective ‘flavour’ magnetic moment  $\mu_{eff}$ .  $\mu_{eff}$  is influenced by mixing of the neutrino magnetic moments (and electric moments) expressed in the mass basis (as described above) and neutrino oscillations **TO DO: This basis relation was already partly described above, mention that and combine the descriptions.** In the ultra-relativistic limit, the neutrino effective magnetic moment is

$$\mu_{\nu_i}^2 (L, E_\nu) = \sum_j \left| \sum_k U_{lk}^* e^{\mp i \Delta m_{kj}^2 L / 2E_\nu} (\mu_{jk} - i\epsilon_{jk}) \right|^2, \quad (1.13)$$

where the minus sign in the exponent is for neutrinos and the plus sign for antineutrinos [2]. Therefore the only difference between the effective neutrino and antineutrinos magnetic moment is in the phase induced by neutrino oscillations.

For experiments with baselines short enough that neutrino oscillations would not have time to develop ( $\Delta m^2 L / 2E_\nu \ll \sim 1$ ), such as the NuMI Off-axis  $\nu_e$  Appearance

(NOvA) Near Detector (ND), the effective magnetic moment can be expressed as

$$\mu_{\nu_l}^2 = \mu_{\bar{\nu}_l}^2 \simeq \sum_j \left| \sum_k U_{lk}^* (\mu_{jk} - i\epsilon_{jk}) \right|^2 = [U (\mu^2 + \epsilon^2) U^\dagger + 2 \text{Im} (U \mu \epsilon U^\dagger)]_{ll'}, \quad (1.14)$$

which is independent of the neutrino energy **TO DO: Figure out how does this relate to the mag moment cross section which does depend on the neutrino energy!**

**TO DO: Consider if this paragraph is actually important** Since the effective magnetic moment depends on the flavour of the studied neutrino, it is different (but related) for neutrino experiments studying neutrinos from different sources. Additionally some experiments, namely solar neutrino experiments, need to include matter effects on the neutrino oscillations. Therefore the reports on the value (or upper limit) of the effective neutrino magnetic moment are not directly comparable between different types of neutrino experiments. Theorists publish papers trying to extrapolate the measured effective magnetic moments to each neutrino flavour, but necessarily apply assumptions that might not hold in all **BSM** theories.

### 1.1.2 Other neutrino electromagnetic properties

**COMMENT: I am not going to report results on these, so should I even mention them here? Maybe it's enough to just mention that they exist in the intro section... TO DO: This section is not finished, most of this text is just copied from some theory papers for now**

**TO DO: See also StatusAndPerspectiveOfNuMM2016.pdf**

Neutrino electric charge is heavily constraint by the measurements on the neutrality of matter (since generally neutrinos having an electric charge would also mean that neutrons have charge which would affect all heavier nuclei). It is also constrained by the SN1987A, since neutrino having an effective charge would lengthen its path through the extragalactic magnetic fields and would arrive on earth later. It can also be obtained from nu-on-e scatter from the relationship between neutrino millicharge and magnetic moment. [nuElmagInt2015.pdf - sec. VIIA] **TO DO: Make this description shorter, just a single sentence and combine with the charge radius**

The neutrino charge radius is determined by the second term in the expansion of the neutrino charge form factor and can be interpreted using the Fourier transform of

a spherically symmetric charge distribution. It can also be negative since the charge density is not a positively defined quantity. In the SM the charge radius has the form of (possible other definitions exist)

$$\langle r_{\nu_l}^2 \rangle_{SM} = \frac{G_F}{4\sqrt{2}\pi^2} \left[ 3 - 2 \log \left( \frac{m_l^2}{m_W^2} \right) \right]. \quad (1.15)$$

This corresponds to  $\langle r_{\nu_\mu}^2 \rangle_{SM} = 2.4 \times 10^{-33} \text{ cm}^2$  and similar scale for other neutrino flavours. [nuElmagInt2015.pdf - sec. VIIIB]

[nuElmagInt2015.pdf - sec. VIIIB] The effect of the neutrino charge radius on the neutrino-on-electron scattering cross section is through the following shift of the vector coupling constant (Grau and Grifols, 1986; Degrassi, Sirlin, and VMarciano, 1989; Vogel and Engel, 1989; Hagiwara et al., 1994):

$$g_V^{\nu_l} \rightarrow g_V^{\nu_l} + \frac{2}{3} m_W^2 \langle r_{\nu_l}^2 \rangle \sin^2 \theta_W \quad (1.16)$$

[nuElmagInt2015.pdf - sec. VIIIB] The current experimental limits for muon neutrinos are from **TO DO: check the current exp. limits** Hirsch, Nardi, and Restrepo (2003) who obtained the following 90% C.L. bounds on  $\langle r_{\nu_\mu}^2 \rangle$  from a reanalysis of CHARM-II (Vilain et al., 1995) and CCFR (McFarland et al., 1998) data:

$$-0.52 \times 10^{-32} < \langle r_{\nu_\mu}^2 \rangle < 0.68 \times 10^{-32} \text{ cm}^2 \quad (1.17)$$

In the Standard Model, the neutrino anapole moment is somehow coupled with the neutrino charge radii and is functionally identical. the phenomenology of neutrino anapole moments is similar to that of neutrino charge radii. Hence, the limits on the neutrino charge radii discussed in Sec. VII.B also apply to the neutrino anapole moments multiplied by 6. in the standard model the neutrino charge radius and the anapole moment are not defined separately and one can interpret arbitrarily the charge form factor as a charge radius or as an anapole moment. Therefore, the standard model values for the neutrino charge radii in Eqs. (7.35)–(7.38) can be interpreted also as values of the corresponding neutrino anapole moments. [nuElmagInt2015.pdf - sec. VIIIC]

It is possible to consider the toroidal dipole moment as a characteristic of the

neutrino which is more convenient and transparent than the anapole moment for the description of T-invariant interactions with nonconservation of the P and C symmetries. the toroidal and anapole moments coincide in the static limit when the masses of the initial and final neutrino states are equal to each other. The toroidal (anapole) interactions of a Majorana as well as a Dirac neutrino are expected to contribute to the total cross section of neutrino elastic scattering off electrons, quarks, and nuclei. Because of the fact that the toroidal (anapole) interactions contribute to the helicity preserving part of the scattering of neutrinos on electrons, quarks, and nuclei, its contributions to cross sections are similar to those of the neutrino charge radius. In principle, these contributions can be probed and information about toroidal moments can be extracted in low-energy scattering experiments in the future. Different effects of the neutrino toroidal moment are discussed by Ginzburg and Tsytovich (1985), Bukina, Dubovik, and Kuznetsov (1998a, 1998b), and Dubovik and Kuznetsov (1998). In particular, it has been shown that the neutrino toroidal electromagnetic interactions can produce Cherenkov radiation of neutrinos propagating in a medium.

[nuElmagInt2015.pdf - sec. VIIC]

### 1.1.3 Measuring neutrino magnetic moment

The most sensitive method to measure neutrino magnetic moment is the low energy elastic scattering of (anti)neutrinos on electrons [2]. The diagram for this interaction is shown in Fig. 1.2 displaying the two observables, the recoil electron's kinetic energy ( $T_e = E_{e'} - m_e$ ) and the recoil angle with respect to the incoming neutrino beam ( $\theta$ ).

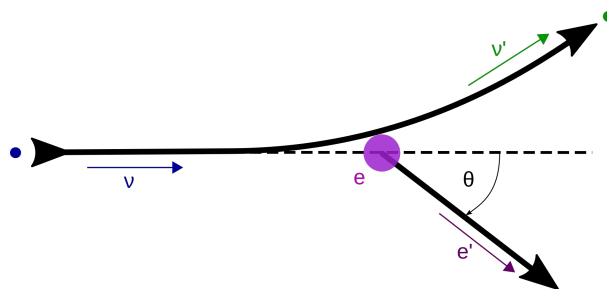


Figure 1.2: Neutrino-on-electron elastic scattering diagram

**COMMENT:** *Is this derivation too trivial to mention in a thesis? Should I just mention the results? I wanted to have this in the technote, but probably too detailed for a*

*thesis... TO DO: Also change all we to passive voice - or should I keep we here?* From simple  $2 \rightarrow 2$  kinematics we can calculate

$$(P_\nu - P_{e'})^2 = (P_{\nu'} - P_e)^2, \quad (1.18)$$

$$m_\nu^2 + m_e^2 - 2E_\nu E_{e'} + 2E_\nu p_{e'} \cos \theta = m_\nu^2 + m_e^2 - 2E_{\nu'} m_e. \quad (1.19)$$

Using the energy conservation

$$E_\nu + m_e = E_{\nu'} + E_{e'} = E_{\nu'} + T_e + m_e \Rightarrow E_{\nu'} = E_\nu - T_e \quad (1.20)$$

we get

$$E_\nu p_{e'} \cos \theta = E_\nu E_{e'} - E_{\nu'} m_e = E_\nu (T_e + m_e) - (E_\nu - T_e) m_e = T_e (E_\nu + m_e), \quad (1.21)$$

$$\cos \theta = \frac{E_\nu + m_e}{E_\nu} \sqrt{\frac{T_e^2}{E_{e'}^2 - m_e^2}} = \frac{E_\nu + m_e}{E_\nu} \sqrt{\frac{T_e^2}{T_e^2 + 2T_e m_e}}. \quad (1.22)$$

And finally we get

$$\cos \theta = \frac{E_\nu + m_e}{E_\nu} \sqrt{\frac{T_e}{T_e + 2m_e}}. \quad (1.23)$$

We can rearrange the Eq. 1.23 to get

$$T_e = \frac{2m_e E_\nu^2 \cos^2 \theta}{(E_\nu + m_e)^2 - E_\nu^2 \cos^2 \theta}. \quad (1.24)$$

Electron's kinetic energy is therefore kinematically constrained by the energy conservation as

$$T_e \leq \frac{2E_\nu^2}{2E_\nu + m_e}, \quad (1.25)$$

which corresponds to the  $\cos \theta \rightarrow 1$  when the recoil electron goes exactly forward in the incident neutrino direction.

Considering  $E_\nu \sim \text{GeV}$ , we can approximate  $\frac{m_e^2}{E_\nu^2} \rightarrow 0$  and from Fig.1.3 we can see that we can approximate all recoil angles to be very small, therefore  $\theta^2 \cong (1 - \cos^2 \theta)$ .

Using Eq.1.23 we get

$$T_e \theta^2 \cong T_e \left( 1 - \left( \frac{E_\nu + m_e}{E_\nu} \right)^2 \frac{T_e}{T_e + 2m_e} \right) = T_e \left( 1 - \left( 1 + \frac{2m_e}{E_\nu} \right) \frac{T_e}{T_e + 2m_e} \right), \quad (1.26)$$

therefore

$$T_e \theta^2 \cong \frac{2m_e T_e}{T_e + 2m_e} \left( 1 - \frac{T_e}{E_\nu} \right) = 2m_e \left( \frac{1}{1 + \frac{2m_e}{T_e}} \right) \left( 1 - \frac{T_e}{E_\nu} \right), \quad (1.27)$$

and finally

$$T_e \theta^2 \cong 2m_e \left( 1 - \frac{T_e}{E_\nu} \right) < 2m_e. \quad (1.28)$$

This is a strong limit that clearly distinguishes the neutrino-on-electron ( $\nu$ -on-e) elastic scattering events from other similar interaction involving single electron (mainly the  $\nu_e$  Charged Current (CC) interaction).

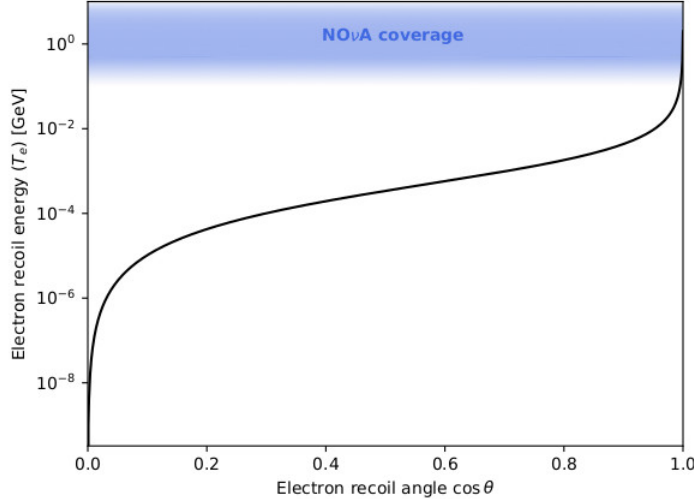


Figure 1.3: Relation between the recoil electron's kinetic energy and angle for  $\nu$ -on-e elastic scattering. The coverage of the NOvA detectors for measuring the electron recoil energy is shown in blue. Only very forwards electron's are recorded in NOvA.

### Neutrino magnetic moment cross section

**COMMENT:** *Should this only be a subsubsection?* In the ultra-relativistic limit, the neutrino magnetic moment changes the neutrino helicity, turning active neutrinos into sterile **TO DO: cite this properly**. Since the **SM** weak interaction conserves helicity

we can simply add the two contribution to the  $\nu$ -on-e cross section incoherently [2]:

$$\frac{d\sigma_{\nu_l e^-}}{dT_e} = \left( \frac{d\sigma_{\nu_l e^-}}{dT_e} \right)_{SM} + \left( \frac{d\sigma_{\nu_l e^-}}{dT_e} \right)_{MAG}. \quad (1.29)$$

The SM contribution can be expressed as [2]:

$$\begin{aligned} \left( \frac{d\sigma_{\nu_l e^-}}{dT_e} \right)_{SM} &= \frac{G_F^2 m_e}{2\pi} \left\{ (g_V^{\nu_l} + g_A^{\nu_l})^2 + (g_V^{\nu_l} - g_A^{\nu_l})^2 \left( 1 - \frac{T_e}{E_\nu} \right)^2 \right. \\ &\quad \left. + ((g_A^{\nu_l})^2 - (g_V^{\nu_l})^2) \frac{m_e T_e}{E_\nu^2} \right\}, \end{aligned} \quad (1.30)$$

where the coupling constants  $g_V$  and  $g_A$  are different for different neutrino flavours and for antineutrinos. Their values are:

$$g_V^{\nu_e} = 2 \sin^2 \theta_W + 1/2, \quad g_A^{\nu_e} = 1/2, \quad (1.31)$$

$$g_V^{\nu_{\mu,\tau}} = 2 \sin^2 \theta_W - 1/2, \quad g_A^{\nu_{\mu,\tau}} = -1/2. \quad (1.32)$$

For antineutrinos  $g_A \rightarrow -g_A$ .

**TO DO: Decide if this is actually useful or not** Using Eq. 1.24 it is possible to get the differential cross section for  $\cos \theta$ :

$$dT_e = \frac{4m_e E_\nu^2 (m_e + E_\nu)^2}{[(m_e + E_\nu)^2 - E_\nu^2 \cos^2 \theta]^2} \cos \theta d\cos \theta \quad (1.33)$$

as

$$\begin{aligned} \left( \frac{d\sigma_{\nu_l e^-}}{d\cos \theta} \right)_{SM} &= \frac{2G_F^2 E_\nu^2 m_e^2 \cos \theta (E_\nu + m_e)^2}{\pi ((E_\nu + m_e)^2 - E_\nu^2 \cos^2 \theta)^2} \\ &\quad \left\{ (g_V^{\nu_l} + g_A^{\nu_l})^2 + (g_V^{\nu_l} - g_A^{\nu_l})^2 \left( 1 - \frac{2m_e E_\nu \cos^2 \theta}{(E_\nu + m_e)^2 - E_\nu^2 \cos^2 \theta} \right)^2 + \right. \\ &\quad \left. ((g_A^{\nu_l})^2 - (g_V^{\nu_l})^2) \frac{2m_e^2 \cos^2 \theta}{((E_\nu + m_e)^2 - E_\nu^2 \cos^2 \theta)} \right\}, \end{aligned} \quad (1.34)$$

The neutrino magnetic moment contribution is **TO DO: include derivation from [?]** [2]:

$$\left( \frac{d\sigma_{\nu_l e^-}}{dT_e} \right)_{MAG} = \frac{\pi \alpha^2}{m_e^2} \left( \frac{1}{T_e} - \frac{1}{E_\nu} \right) \left( \frac{\mu_{\nu_l}}{\mu_B} \right)^2, \quad (1.35)$$

Table 1.1: Neutrino-on-electron elastic scattering total cross sections. TO DO: *Move units to title and add cross sections with thresholds. Also reference this somewhere in text* from Fundamentals of neutrino Physics and Astrophysics, p.139

Process	Total cross section
$\nu_e + e^-$	$\simeq 93 \times 10^{-43} E_\nu \text{cm}^2 \text{GeV}^{-1}$
$\bar{\nu}_e + e^-$	$\simeq 39 \times 10^{-43} E_\nu \text{cm}^2 \text{GeV}^{-1}$
$\nu_{\mu,\tau} + e^-$	$\simeq 15 \times 10^{-43} E_\nu \text{cm}^2 \text{GeV}^{-1}$
$\bar{\nu}_{\mu,\tau} + e^-$	$\simeq 13 \times 10^{-43} E_\nu \text{cm}^2 \text{GeV}^{-1}$

where  $\alpha$  is the fine structure constant TO DO: *Calculate the total mag moment cross sections.*

Comparison of the SM and the neutrino magnetic moment cross sections is shown on Fig.1.4. Whereas the SM cross section is flat with  $T_e \rightarrow 0$ , the neutrino magnetic moment cross section keeps increasing to infinity. However, this reach is limited by the experimental capabilities of detecting such low energetic neutrinos. Possible NOvA coverage is shown in a shaded blue and it is uncertain we could actually reach as low as 100 MeV TO DO: *Change this claims a little bit.*

As can be seen in Fig. 1.4 and Fig. 1.5, the magnetic moment contribution exceeds the SM contribution for low enough  $T_e$ . This can be approximated as [2]:

$$T_e \lesssim \frac{\pi^2 \alpha^2}{G_F^2 m_e^3} \left( \frac{\mu_\nu}{\mu_B} \right)^2 \simeq 2.9 \times 10^{19} \left( \frac{\mu_\nu}{\mu_B} \right)^2 [\text{MeV}], \quad (1.36)$$

which does not depend on the neutrino energy and makes experiments sensitive to lower energetic electrons more sensitive to the neutrino magnetic moment. This is especially true for the recent dark matter experiments which put stringent limits on the solar neutrino effective magnetic moment, as described in the following section.

## 1.2 Experimental overview

COMMENT: *Should I include cosmological implication here?* TO DO: *Describe the limits from other experiments*

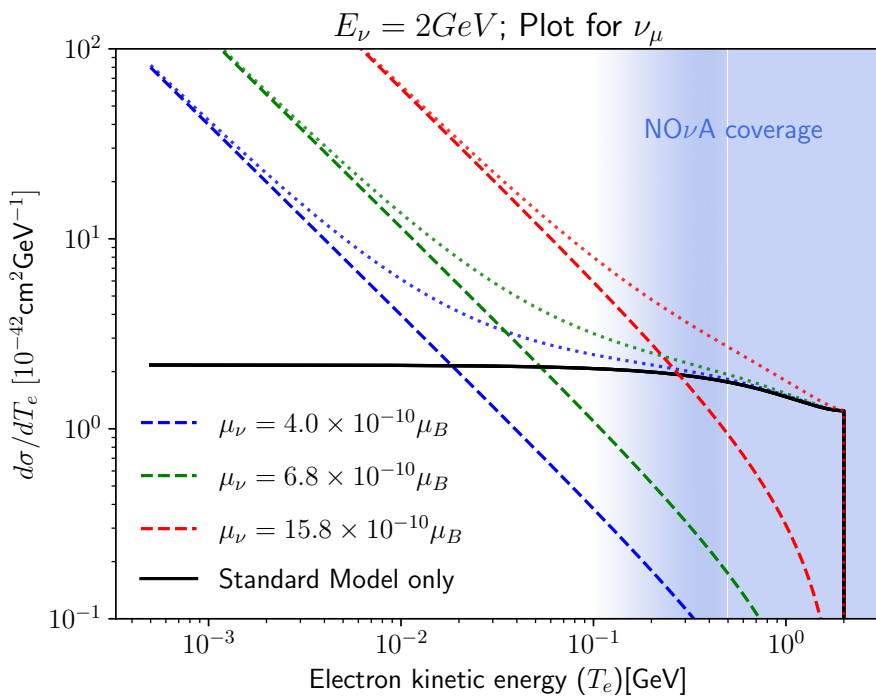


Figure 1.4: Comparison of the neutrino magnetic moment (coloured) and the SM (black) cross sections for the  $\nu$ -on-e elastic scattering. Different colours depict different values of the neutrino magnetic moment. Dashed lines are the individual cross sections and dotted lines are the added total cross section with the standard model contribution. NOvA coverage of electron recoil energies is shown in shaded blue TO DO: Reference the colours on the figures to the origins of the values (LSND and Biao).

$E_\nu = 2\text{GeV}$ ; Plot for  $\nu_\mu$

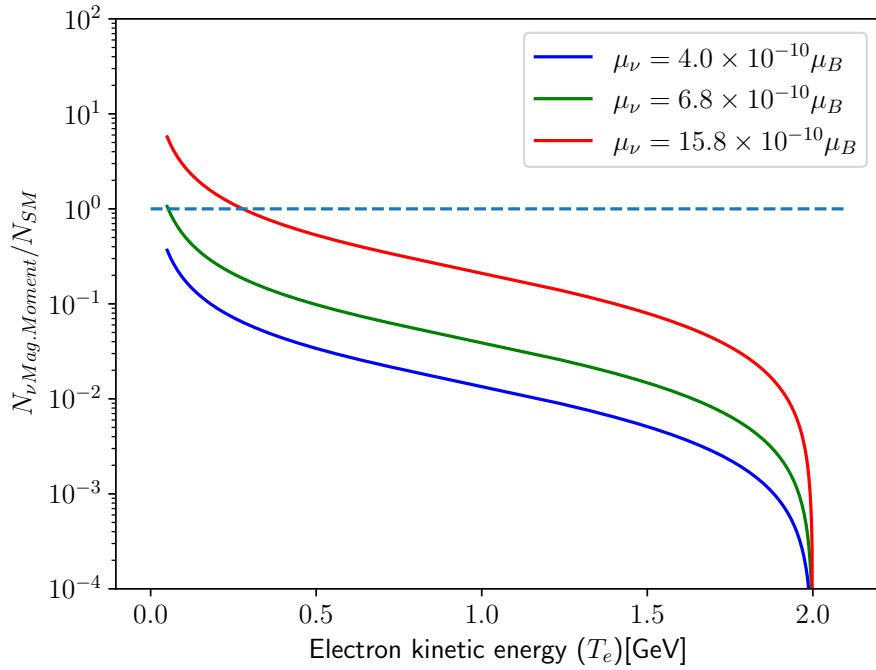


Figure 1.5: Ratio of the neutrino magnetic moment cross section to the SM cross section for the  $\nu$ -on-e elastic scattering. Different colours depict different effective muon neutrino magnetic moment values.

### 1.3 Analysis overview

In this analysis we are searching for a signal of possible neutrino magnetic moment events in the NOvA ND. This signal would manifest as an excess of  $\nu$ -on-e elastic scattering events at low electron recoil energies on top of the SM background, as described in Sec. 1.1.3. In case we would not observe any excess (null hypothesis), we would provide an upper limit on the effective muon neutrino magnetic moment.

The  $\nu$ -on-e interactions are also used in the ND group's analysis to constraint the neutrino beam prediction [?], which relies on the precise theoretical knowledge of the  $\nu$ -on-e interaction cross section. They compare the total number of recorded  $\nu$ -on-e interactions, with background subtracted based on a comparison of data and simulation in a sideband region, to the prediction. Since the number of  $\nu$ -on-e events should only depend on the normalization of the neutrino beam, this analysis should give us a precise validation, or correction, of the neutrino flux normalization. There has been a large amount of work going into this analysis, including making special samples, weights, event classifiers, developing a dedicated event selection, or developing a background subtraction method, among others. To save time and analysis

effort, we have taken most of these work at face value and applied it to the neutrino magnetic moment analysis. This will help us get the first good estimate of **NOvA**'s capabilities to constraint (or measure) the neutrino magnetic moment.

The same detector signature of a single forward going electron shower, as present in the  $\nu$ -on-e events, is also present in the Light Dark Matter (LDM) analysis [? ]. This analysis is using a similar event selection to select the LDM events as the ND group, only without the final  $E\theta^2$  cut (see Sec.??). However, instead of simply comparing the total event counts, the LDM analysis is using a CAFAna-based fitting framework to fit for the possible LDM signal in a distribution of electron recoil energy multiplied by electron recoil angle squared.

Our analysis strategy is to compare the recorded number of neutrino events in data with a predicted number of signal events, which depends on the neutrino magnetic moment value, on top of a SM background. We use the ND group's sideband region to constraint the non- $\nu$ -on-e background with data. It is also possible to use a second sideband sample, based on the electron recoil energy, to provide an additional constraint on the  $\nu$ -on-e background, but this idea has not been visited yet.

In the future, this analysis can be improved for example by improving the event selection, creating additional background samples, by including antineutrino events, or by using using a fit to the energy distribution, similarly to the LDM analysis.

This section describes the simulation samples used to predict the number of signal and background events (Sec.1.3.1) and the weights used to correct for known limitations of the simulation (Sec. 1.3.2).

### 1.3.1 Datasets and Event Reconstruction details

For this analysis we are using near detector CAF samples with the standard Production 5.1 reconstruction.

We are following the standard data blinding procedure and have not looked at any data events until the analysis passes the full collaboration review. The Near Detector group has validated TO DO: *Figure out where did Yiwen and Wenjie actually look at the data* using this data sample.

The exposure of the data sample is approximately  $1.3848600 \times 10^{21}$  POT. This is the exposure we use for all the following studies shown in this technical note.

The Prod5.1 ND data sample contains data from run 10391 in epoch1a (2014-08-22 21:08:40) until run 14010 in epoch 11a (2021-02-03 15:48:21) (from the period and epoch naming wiki page [https://cdcv.s.fnal.gov/redmine/projects/novaart/wiki/Period\\_and\\_Epoch\\_Naming](https://cdcv.s.fnal.gov/redmine/projects/novaart/wiki/Period_and_Epoch_Naming))

**TO DO:** *Briefly describe the MC details. Versions of the individual simulation software*

To tackle the low number of  $\nu$ -on-e and  $\nu_e$ CC Meson Exchange Current (MEC) events in the nominal simulation sample we are using a suit of nominal and enhanced simulation samples for four different signal and background components. Each one contains its nominal sample and special systematically shifted samples for the detector systematics. The use of the samples is summarised in table 1.4 and described in detail below.

The GENIE tune is GENIE N1810j 02 11a (from the Prod5.Frankenstein docdb: 53360). The Genie release used for this production is R20-08-06-prod5.1genie.h, which has GENIE version V3.0.6 [? ]

Also prod5.1 uses Geant4 v4.10.4.p02 [? ]

We use the standard NOvA simulation (reference NOvA 3fl paper DOI: 10.1103/PhysRevD.106.032004)

Describe how did we deal with the GENIE skew fix. It was the GSF weights that forces "us" to treat the nueCC MEC background differently than the other background. As I understand it, the GSF is applied simply as the new weight. No change to the systematics is required.

Reference: A. Mislavic, "Genie skew reweight validation." NOvA Internal Document, DocDB: 553811 [from antinueCC IncXSec docdb:53691] "Final state kinematics were predicted by the N1810j 00 000 tune, but total cross section were generated with the intended N1810j 0211a179 tune, which differed in RES and DIS rates tuned to external data. Properly correcting the skew180 would require all simulation to be regenerated, so a temporary solution developed by the NOvA181 Cross-section Tuning Group involves reweighing production 5.1 events to the default N1810j 00 000.182 An additional modification to the GENIE MEC contribution are applied to better agree with NOvA183 ND data.

MC includes simulation in the rock surrounding the ND

**TO DO:** *Describe here that we're using the nominal ND MC sample for signal utilization*

*ing the simple relationship between the Standard Model cross section and the neutrino magnetic moment cross section (ref. theory)*

The signal of the neutrino magnetic moment analysis is just a re-weighted signal of the  $\nu$ -on-e analysis from the near detector group. We are using the same event selection as the near detector group.

*TO DO: Say already here that the POT inside the enhanced MC samples are not properly accounted for in CAFAna (Loader issue) and so the event counts need to be adjusted post-hoc*

Table 1.2: Overview of the simulation samples corresponding to different signal and background components.

Signal	Enhanced $\nu$ -on-e sample
$\nu$ -on-e background	Enhanced $\nu$ -on-e sample
$\nu_e$ CC MEC background	Enhanced $\nu_e$ CC MEC sample
Other background	Nominal ND CAF sample

### **Enhanced $\nu$ -on-e sample**

*TO DO: Describe the nuone sample* Created by Wenjie Wu (was it just him or also Yiwen?) to do ... and fully described in the technote [? ]. Using the overlayed and filematched samples for consistency.

Incorrect POT is 3.6995434e+20, Correct POT is 1.7209423e+24 (this should be filematched)

*TO DO: Find a reference and reasoning for why Wenjie hasn't created the other systematics samples* We only have the selected few systematics definitions because ...

*TO DO: Describe the differences*

- Missing cross section parameters - unable to use cross section weights or so
- Special mode for nu-on-e elastic scattering 10005

### **Enhanced $\nu_e$ CC MEC sample**

Created by Yiwen Xiao [? ] to tackle the low statistics of the  $\nu_e$ CC MEC background events and subsequently large and unphysical cross section weights.

Incorrect POT is 4.7334120e+23 and correct POT is 1.9880340e+24. This is filematched

**TO DO:** *List the limitations of the sample in the  $q_3$ - $q_0$  parameter space*

### Near Detector filematched CAF sample

**TO DO:** *describe all the ND nominal CAF samples* **TO DO:** *Also mention the decaf sample and discuss if we could use them or not*

The nominal ND MC includes 4x data POT. The systematics are file-matched to remove any statistical bias

Total POT is 5.54497e+21 But for the filematched samples (batch 2) there's only 1.93109e+21

### 1.3.2 Analysis weights

**TO DO:** *Describe why do we use weights* What are the weights we are using and why?

To correct for known deficiencies in simulation of neutrino flux or cross sections we apply weights calculated for each event.

Table 1.3 shows what CAFAna weights are used to simulate what signal/background sample.

Table 1.3: Overview of CAFAna weights applied to each analysis sample.

Signal	Flux and neutrino magnetic moment weights
$\nu$ -on-e background	Flux and radiative correction weights
$\nu_e$ CC MEC background	Flux and cross section weights
Other background	Flux and cross section weights

### PPFX weight

ana::kPPFXFluxCVWgt [? ] **TO DO:** *What does this do (one sentence ish).* Maybe cite Leo's thesis? Or paper? L. Aliaga, "Neutrino Flux Prediction for the NuMI Beamline." PhD Thesis, FERMILAB-1081 THESIS-2016-03

### Prod5.1 GSF XSec weight

ana::kXSecCVWgt2020GSFProd51 **TO DO:** *Find the reference: possibly Maria's docdb:53336 together with the official 2020 XSec tuning technote docdb:43962.*

NOvAReweighting reference: J. Wolcott, “NOvARwgt software.” <https://github.com/novaexperiment/NOvARwgt> public.

*TO DO: Briefly describe what does this do. Also mention Yiwen’s talk/technote about the large XSec weights that made her create an enhanced nueCC MEC sample.*

We are only using the for the background since we assume that the cross section for the signal is perfect. Also there are no weights for this kind of interaction.

## Radiative correction weight

*TO DO: Why are we doing this? (reference Yiwen’s talk/technote).*

Mention here where did I get the original GENIE cross section from (reference Yiwen’s talk or technote, plus the original paper that was used). nu-on-e technote[?] ]

*TO DO: Write out the actual version of the weight. Including the original and the corrected XSec constants*

MINERvA paper: <https://journals.aps.org/prd/pdf/10.1103/PhysRevD.100.092001>

Say that we are not using the third part of the correction because it is tiny and it makes no difference. (tried and tested)

*TO DO: correct the equation* Calculated as

$$\text{weight}_{\text{Radiative Corr.}} = \frac{d\sigma_{\nu-\text{on}-e}}{dy} \Big|_{\text{Radiative Corr.}} / \frac{d\sigma_{\nu-\text{on}-e}}{dy} \Big|_{\text{GENIE 3}} ; y = \frac{E_e - m_e}{E_\nu} \quad (1.37)$$

## Neutrino magnetic moment signal as a weight

*TO DO: What does this do and why does it work? Reference the theory part as to why is the magnetic moment signal simply a rescaling of the GENIE cross section.*

Using the same tree-level cross section from GENIE as in the rad. corr. weight.

*TO DO: Write the name of the weight in CAFAna/nuone namespace and where it is located*

*TO DO: correct the equation* Calculated as

$$\text{weight}_{\nu \text{ Mag. Moment}} = \frac{d\sigma_{\nu-\text{on}-e}}{dy} \Big|_{\nu \text{ Mag. Moment}} / \frac{d\sigma_{\nu-\text{on}-e}}{dy} \Big|_{\text{GENIE 3}} ; y = \frac{E_e - m_e}{E_\nu} \quad (1.38)$$

## 1.4 Event selection

Mention what are the main backgrounds for this analysis. They would be the events that produce electromagnetic showers: electrons or gamma in the final state. This can be the beam nueCC, or events that produce  $\pi^0$ , either CC or NC.

We are trying to select low energy neutrino-on-electron events, which are characterised by a single very forward going electron shower. Since these are the same events as are used in the ND group's analysis to constraint the neutrino beam prediction with a  $\nu\text{-on-e}$  events [?], we have taken their event selection without changes. This is to save time and analysis efforts, but also to get a first good estimation of NOvA's capabilities to constraint (or measure) neutrino magnetic moment. Almost the same selection is also used in the LDM analysis [?], only without the final  $E\theta^2$  cut.

We explain the motivation behind each cut of the event selection and discuss their effect on the neutrino magnetic moment events below. We also consider possible improvements to the event selection for a future (re-)analysis. TO DO: *Also describe how were the cuts selected*

### Signal Definition

To define the signal and background samples we use the true information listed in Tab. 1.4. The neutrino magnetic moment signal definition is the same as that for the  $\nu\text{-on-e}$  background with the neutrino magnetic moment weight applied (explained in Sec. 1.3.2).

The signal definitions use the kMode variable instead of the kIntType, which is now deprecated (ref.: various Slack conversations). Mode 10005 denotes only the  $\nu\text{-on-e}$  events and is only available for the enhanced  $\nu\text{-on-e}$  samples, while mode 5 denotes all electron scattering events, including inverse muon decay interactions. That is why we had to add a requirement of an electron in the final state. Mode 10 denotes all Meson Exchange Current (MEC) events.

We are using the ND group's [?] signal definition including a requirement for the true vertex to lie within their fiducial volume (defined below). This is the cut name NDNuoneFiducial. This is in contrast with the LDM analysis [?], which uses the ana::kVtxIsContained cut instead, which has a looser boundary. This

choice has only a negligible effect on the final number of selected events and only affects the selection efficiency.

Table 1.4: Overview of signal and background definitions.

Signal	<code>kMode== 10005 &amp;&amp; NDNuoneFiducial</code>
$\nu$ -on-e background	<code>kMode== 10005 &amp;&amp; NDNuoneFiducial</code>
$\nu_e$ CC MEC background	<code>!(kMode== 5 &amp;&amp; kElInFinState &amp;&amp; NDNuoneFiducial) &amp;&amp; (kIsCC &amp;&amp; kIsNue &amp;&amp; kMode == 10)</code>
Other background	<code>!(kMode== 5 &amp;&amp; kElInFinState &amp;&amp; NDNuoneFiducial) &amp;&amp; !(kIsCC &amp;&amp; kIsNue &amp;&amp; kMode == 10)</code>

## Data Quality Selection

Spill cuts To ensure good data quality, we apply the following criteria on the run, subrun and spill level. **TO DO: Add a description of the spill quality cuts (only applied to data)**

## Basic Reconstruction Quality Selection

**TO DO: Split the pre-selection into basic reco quality and basic event selection** Literally taken from the 3 flavour's nue appearance low energy selection Pre-selection cuts include basic quality cuts that remove events with invalid vertex reconstruction and events with no reconstructed prongs, as shown on Fig. 1.6.

[nueXSec ana, docdb:37668] One additional detector issues is the presence of "FEB Flashers" within reconstructed slices. FEB flashers are caused by high energy deposits in one cell, which induces a sagged baseline in all other channels on the same APD. When the baseline is restored, fake hits are triggered on the whole APD.

Requiring at least one reconstructed vertex and at least one reconstructed prong (and shower). Also requiring that there are  $< 8$  hits per plane to remove FEB flashers.

## Basic Event Selection

again Literally taken from the 3 flavour's nue appearance low energy selection

The pre-selection cuts have been kept from the  $\nu_e$ CC analysis with loosened cut values **TO DO: find a reference for this analysis**. They also remove the obvious  $\nu_\mu$ CC

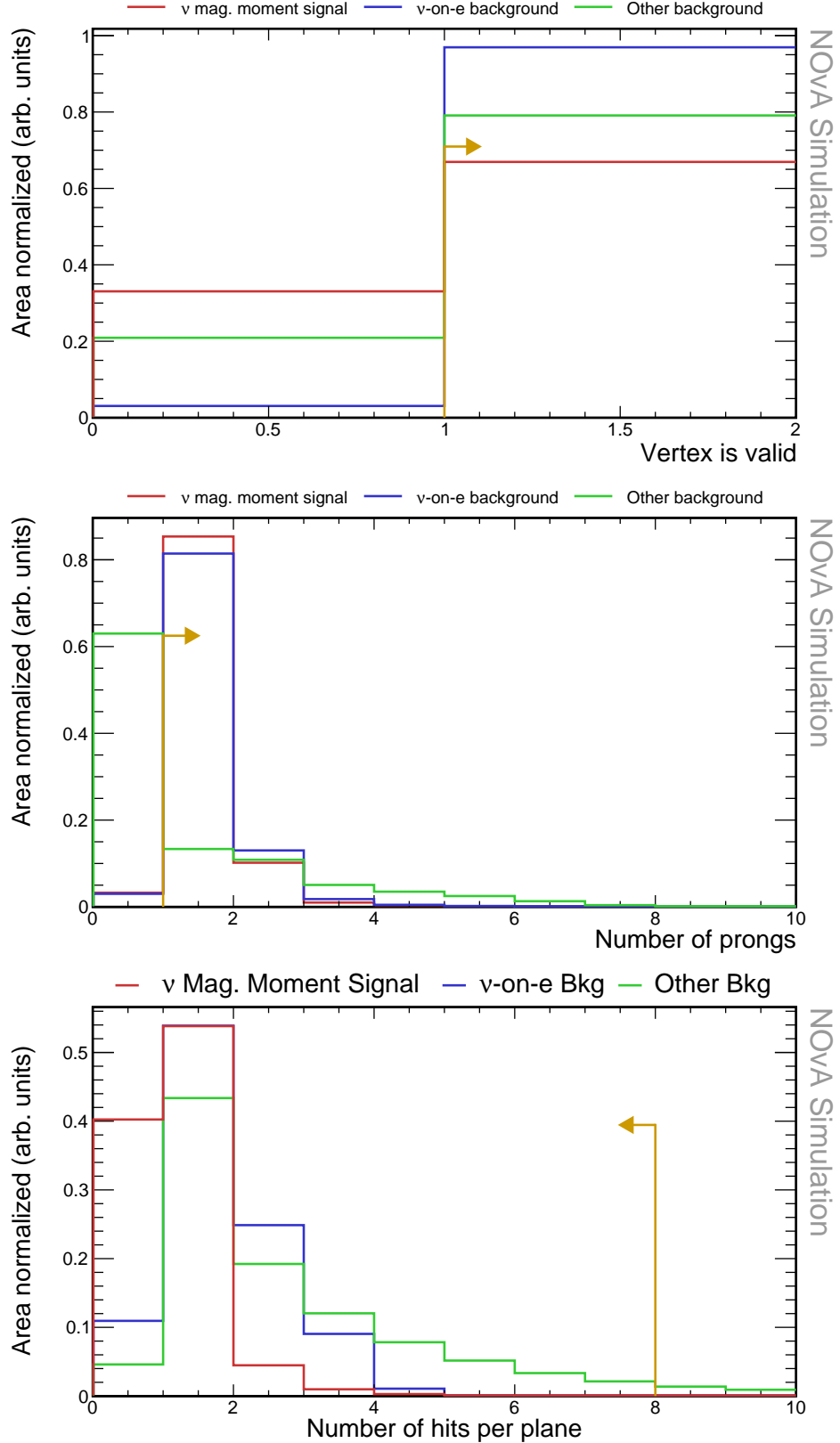


Figure 1.6: Relative comparison of signal,  $\nu$ -on-e background, and other background events for basic reconstruction quality selection variables. No cuts were applied to make these plots. Yellow lines indicate the cut values for the shown variables, with arrows pointing towards the preserved events. All plots show relative comparison with histograms normalised to their areas.

interactions by requiring that the length of the longest prong is  $< 500$  cm and the summed number of cells for all prongs in the slice is  $< 200$ . Relative comparison of signal,  $\nu$ -on-e background, and other background distributions for the pre-selection variables is shown on Fig. ???. This is much stricted than the ND group's  $N\text{Hits} < 600$ ,  $\text{LongestPlane} < 800\text{cm}$  and planes crossed by the longest prong  $< 120$ .

**TO DO:** *Mention that I added a preliminary  $E\theta^2 < 0.04$  cut*

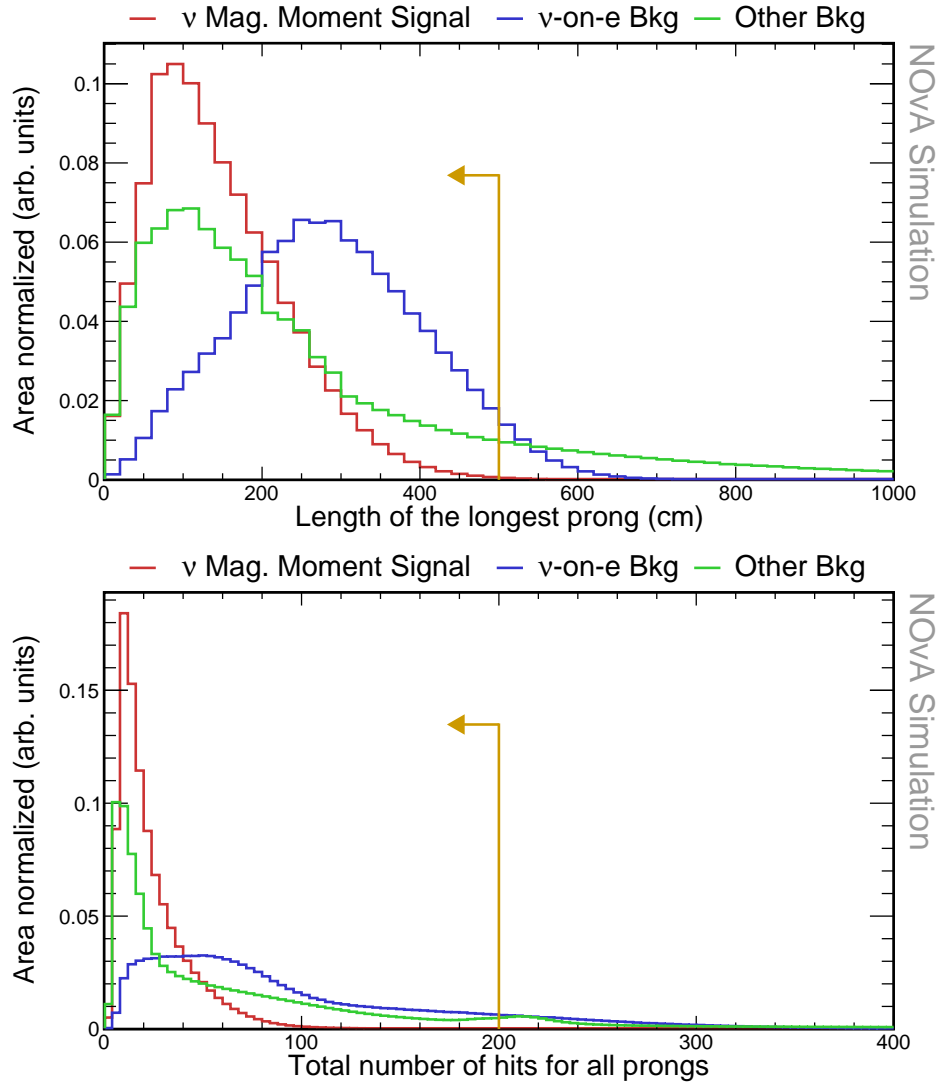


Figure 1.7: Relative comparison of signal,  $\nu$ -on-e background, and other background events for basic pre-selection variables. Cuts on VtxIsValid, number of prongs, and number of hits per plane were applied to make these plots. Yellow lines show the cut values for the shown variables.

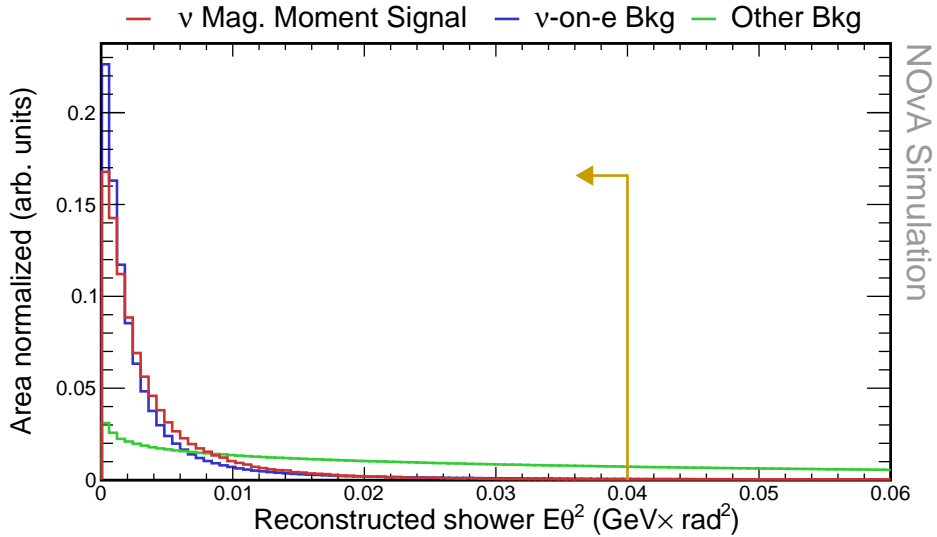


Figure 1.8: Relative comparison of signal,  $\nu$ -on-e background, and other background events for basic pre-selection variables. Cuts on VtxIsValid, number of prongs, and number of hits per plane were applied to make these plots. Yellow lines show the cut values for the shown variables.

### Fiducial and containment cuts

[nueXSec ana, docdb:37668] For both the X and Y vertices the distributions are asymmetric when comparing across the origin, in terms of vertex position. This is primarily due to particles coming from the +y and -x from events in the rock surrounding the detector. This corresponds to the direction of the NuMI target from the near detector. ...We require all activity from neutrino activity be deposited outside of the muon catcher.

**TO DO: *Describe what does the fiducial cut do*** We require that the reconstructed vertex is contained within the following volume:  $-175 < \text{Vtx}_X < 175, -175 < \text{Vtx}_Y < 175, 95 < \text{Vtx}_Z < 1095$  cm.

To ensure all the energy is contained within the detector and to remove events originating outside of the detector (rock muons), we require that the extreme positions of hits for all prongs in the slice are within the following volume:  $-175 < \text{min}_X, \text{max}_X < 175, -175 < \text{min}_Y, \text{max}_Y < 175, 105 < \text{min}_Z, \text{max}_Z < 1270$  cm.

**COMMENT:** *Also made this a bit stricter from the ND group's values as it didn't really make sense*

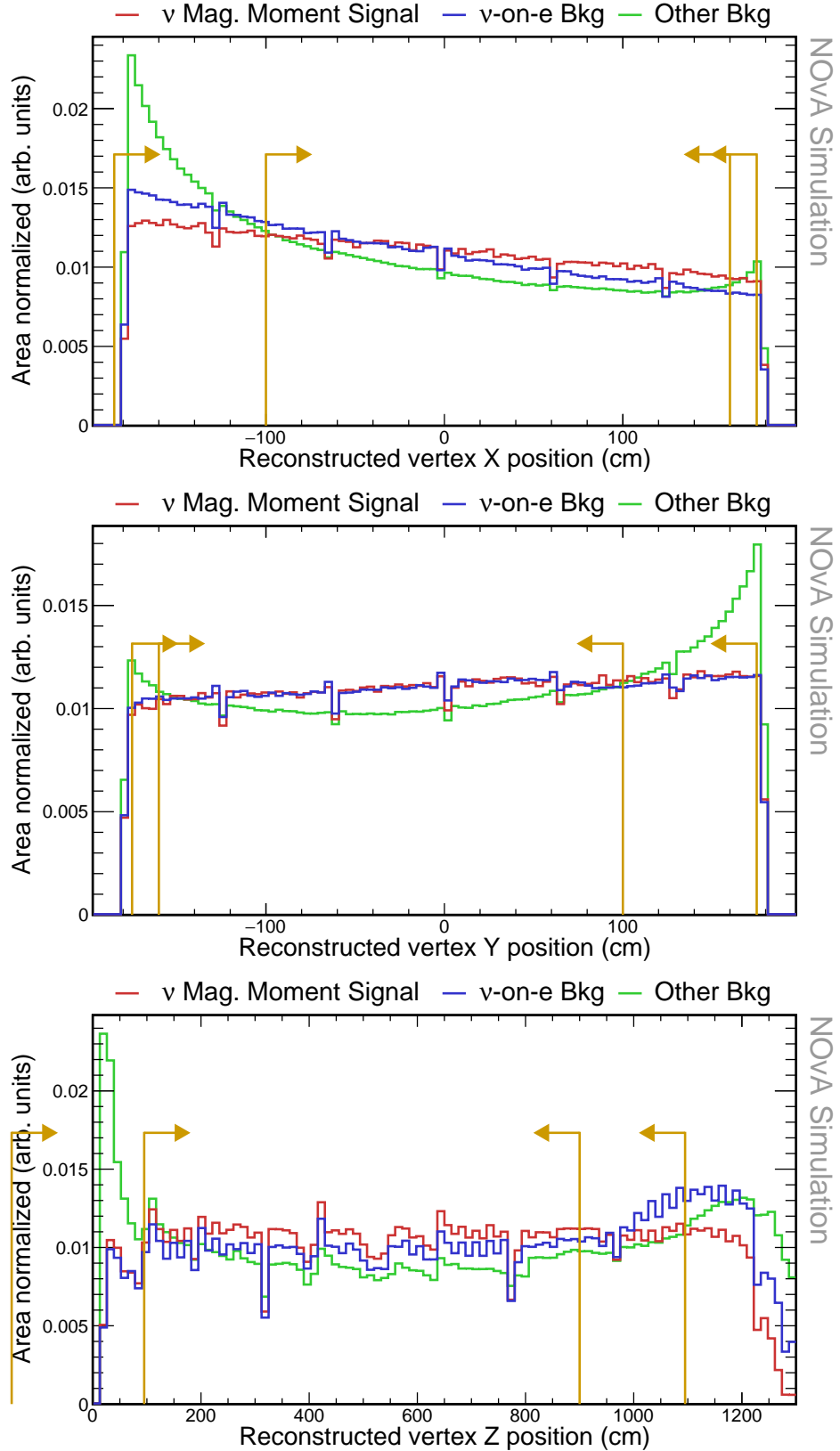


Figure 1.9: Relative comparison of signal,  $\nu$ -on-e background, and other background events for the reconstructed vertex. Basic reconstruction quality and pre-selection cuts were applied prior to making these plots. Additionally, vertex is required to be within the active region of the detector ( $< 1270$  cm) for the two top plots. Gold lines show the cut values that create the fiducial volume.

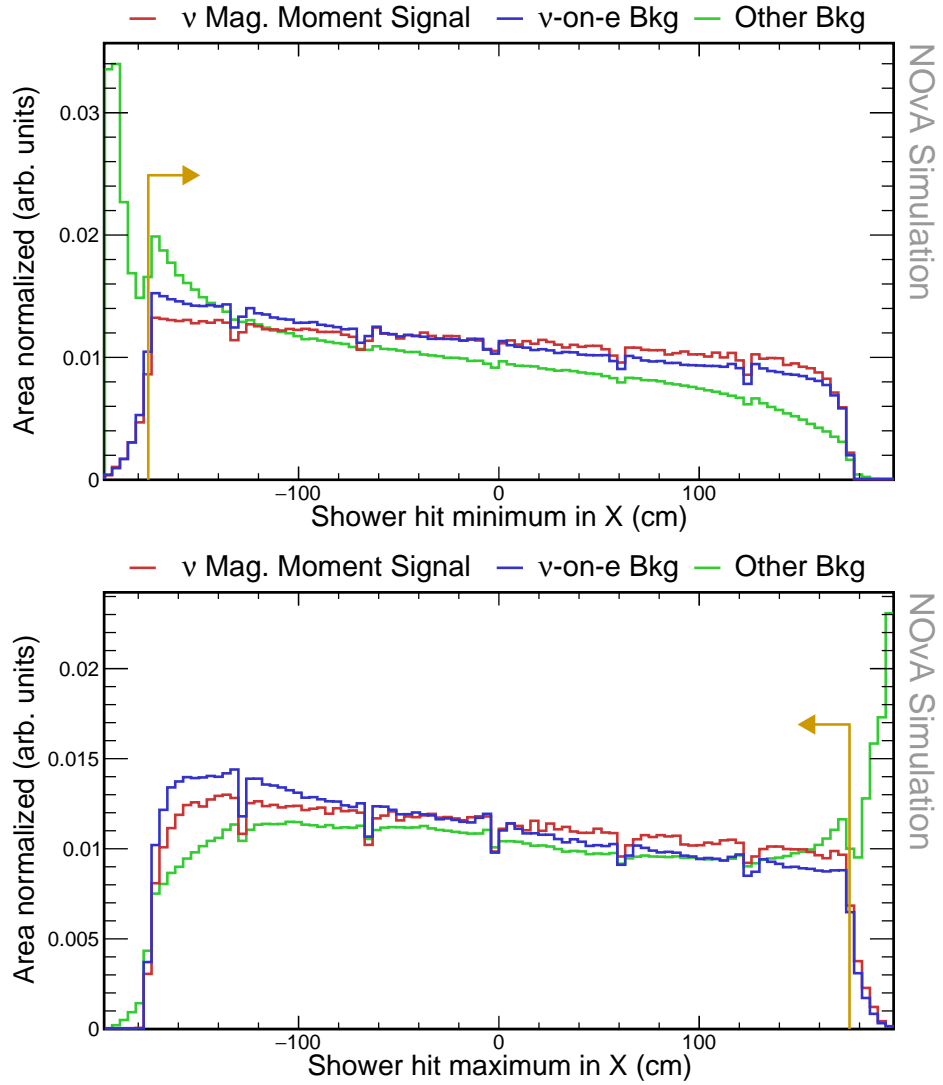


Figure 1.10: Relative comparison of signal,  $\nu$ -on-e background, and other background events for the minimum and maximum position of the reconstructed shower along the x axis. Pre-selection and fiducial cuts were applied to make these plots. Gold lines show the values of the containment cuts.

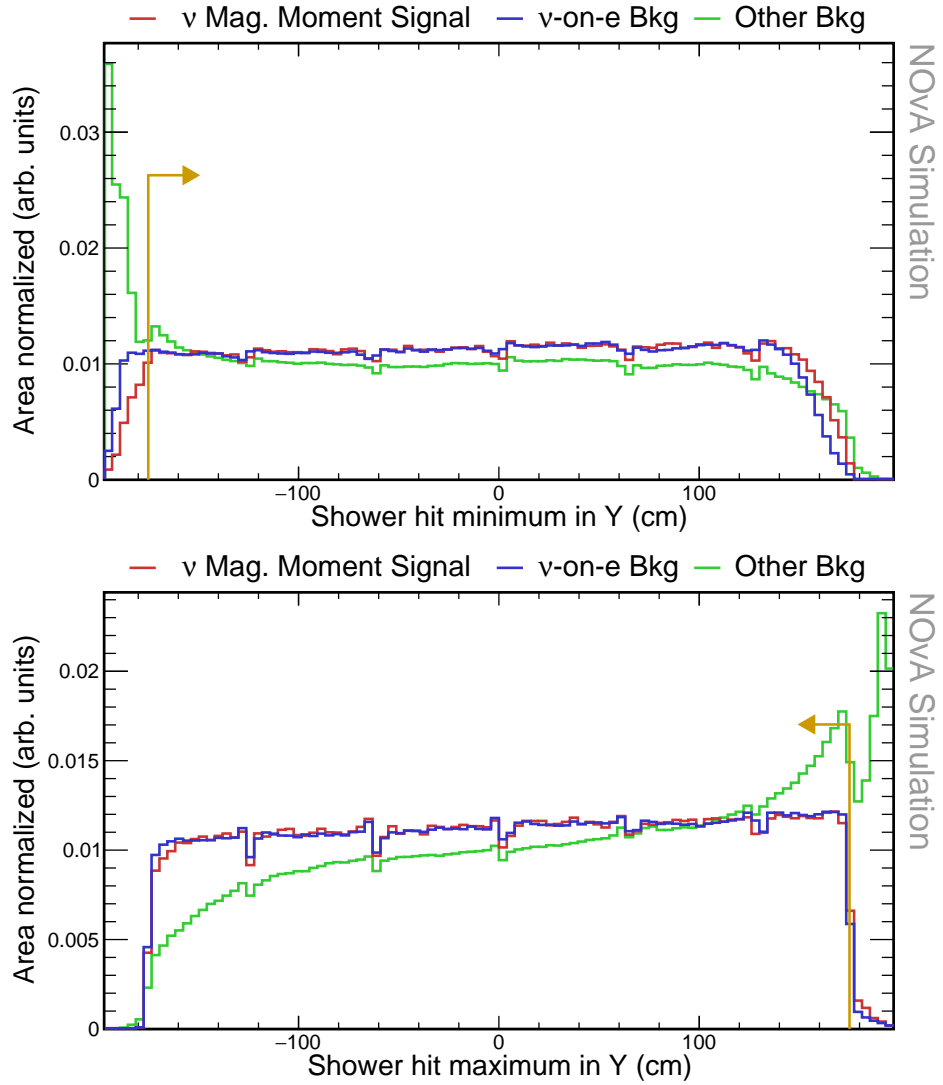


Figure 1.11: Relative comparison of signal,  $\nu$ -on-e background, and other background events for the minimum and maximum position of the reconstructed shower along the Y axis. Pre-selection and fiducial cuts were applied to make these plots. Gold lines show the values of the containment cuts.

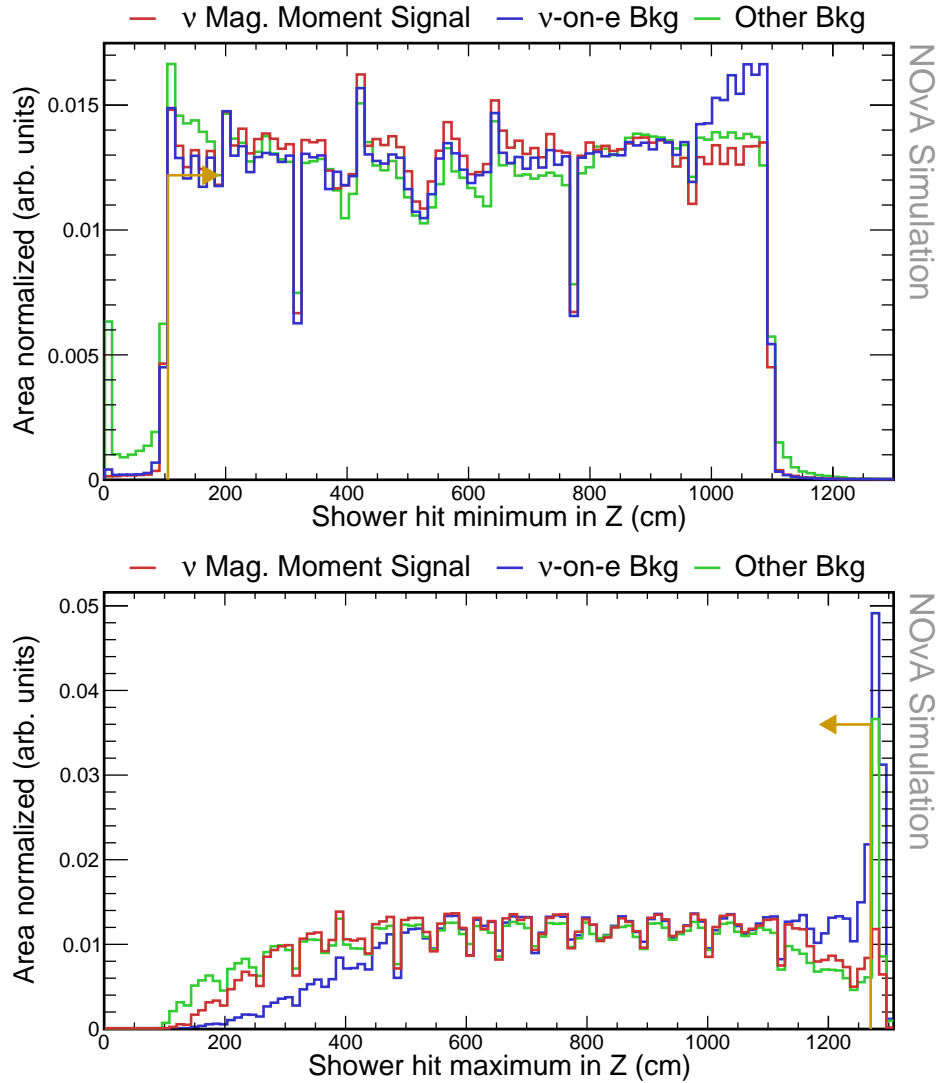


Figure 1.12: Relative comparison of signal,  $\nu$ -on-e background, and other background events for the minimum and maximum position of the reconstructed shower along the Z axis. Pre-selection and fiducial cuts were applied to make these plots. Gold lines show the values of the containment cuts.

### Shower energy cut

COMMENT: Already applying the cut here to help reduce the events for TMVA. This cut is based purely on reco quality (we don't trust events below 0.5GeV, especially not for the CVN nuone ID variables)

TO DO: discuss the energy cut, should this be removed? What is the effect on the event count? Why was this included in the first place (the identifiers are not as strong for lower energies - is this true though? - also there are further unexplored backgrounds that would need to be further studied and explore. Maybe depends on where we move the cut...) The calorimetric energy of the primary shower is required to be within  $0.5 < E_{cal} < 5$  GeV.

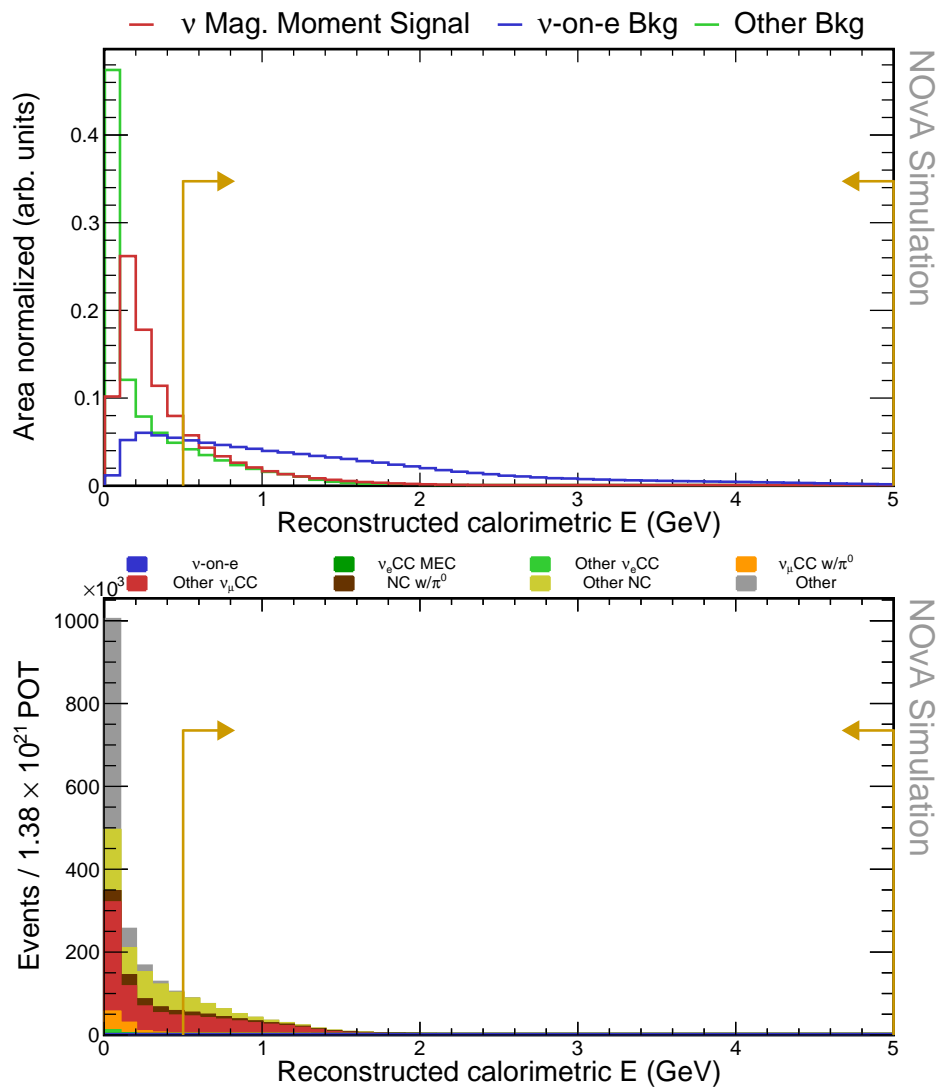


Figure 1.13: Relative comparison of signal,  $\nu$ -on-e background, and other background events for the reconstructed vertex. No cuts were applied to make these plots. Gold lines show the cut values that create the fiducial volume.

## Single particle requirement

**COMMENT:** *This is where I started the TMVA*

To selection events with a single particle we require that the fraction of energy contained in the most energetic shower is  $> 0.8$ , that the summed energy of all cells (above threshold and within  $\pm 8$  planes from the vertex) outside of the most energetic shower is  $< 0.02$  GeV, and that the distance between the vertex and the start of the primary shower is  $< 20$  cm.

## Event classifiers

We are using two event classifiers based on convolution neural network that were developed specifically to identify  $\nu$ -on-e interactions. The first one (Nuone ID) is trained to select  $\nu$ -on-e events and the second one (Epi0 ID) is trained on the events passing the Nuone ID to reject the  $\pi^0$  background. Our selection requires that Nuone ID  $> 0.73$  and that Epi0 ID  $> 0.92$ .

**TO DO:** *reference theory for the kinematics of nuone scattering* We require that the product of reconstructed energy of the primary shower and the square of its angle from the Z axis is  $E_{cal}\theta^2 < 0.005$  GeV  $\times$  rad $^2$ .

**TO DO:** *Add plots of distributions of the event selection variables with two columns. LHS shows no cuts applied and RHS shows all previous cuts applied*

Using the many plots below that show the effect of each of the cuts on the signal and all background events. (For signal we are showing NuMM=...)

**TO DO:** *Describe the cutflow tables below* The final event count and efficiency of each of the cuts is shown on the table 1.5. Table 1.16 shows the dissemination of background into the individual components.

**TO DO:** *Add a discussion of possible improvements on the event selection on its limitations - mostly for the analysis review committee* From here we can see that ... Maybe what can be improved is... This can likely be improved upon by specifically selection low energy events and removing the cut on the reconstructed shower energy.

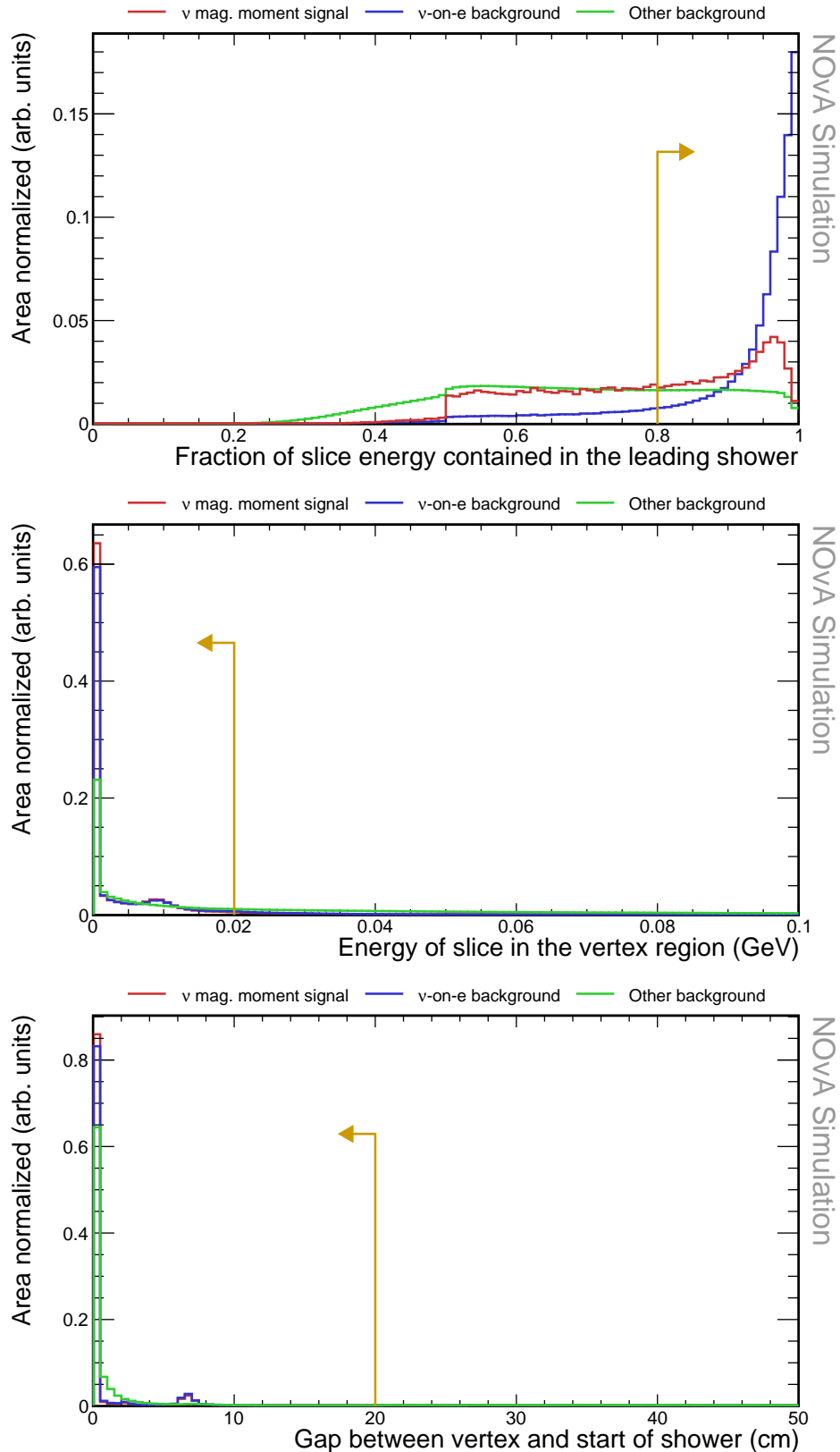


Figure 1.14: OLD Relative comparison of signal,  $\nu$ -on-e background, and other background events for the reconstructed vertex. Every previous cut was applied to make these plots, including the ShwECont for the middle and the bottom plot and the VtxE cut for the bottom plot. Gold lines show the cut values that create the fiducial volume.

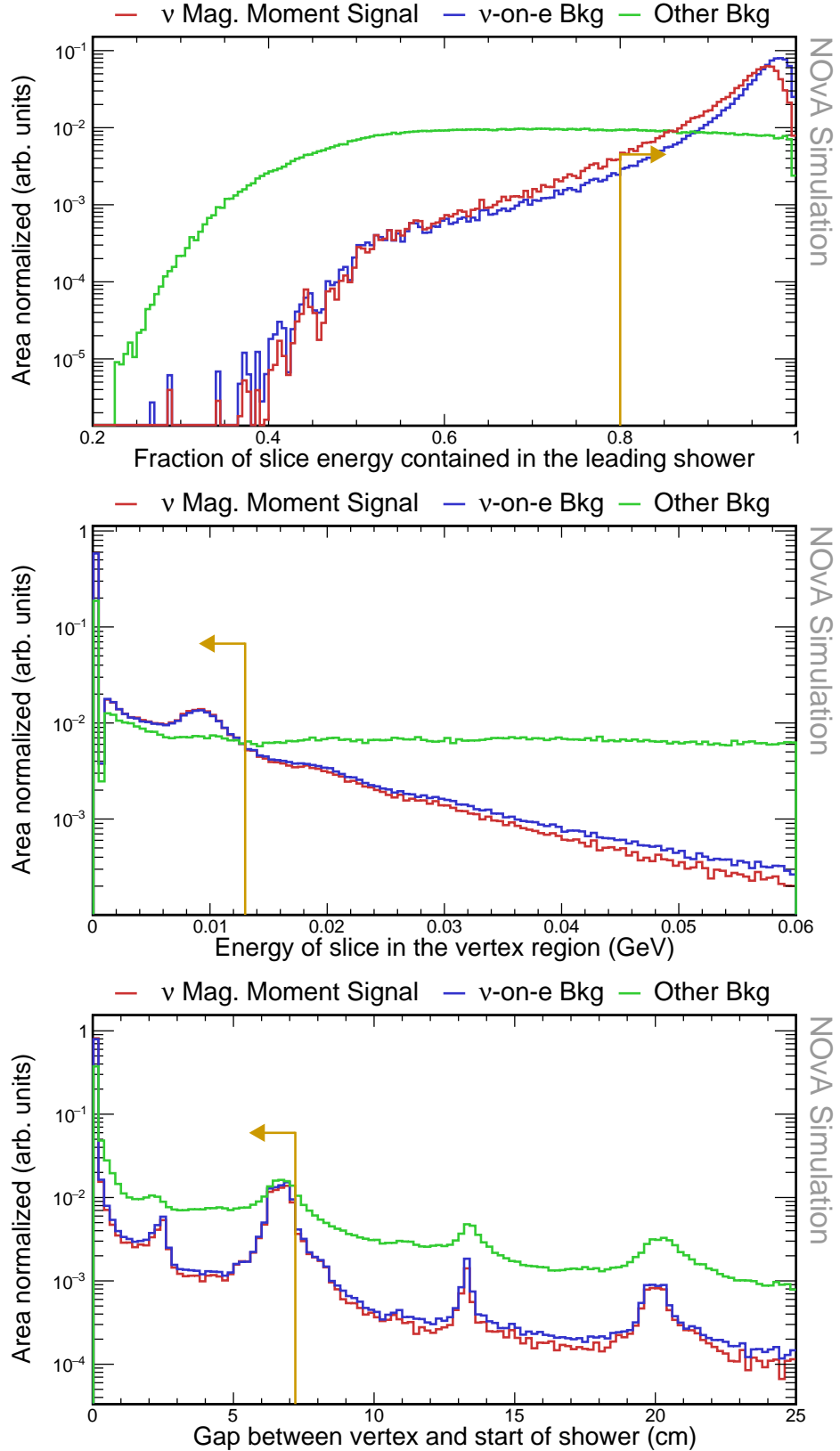


Figure 1.15: Relative comparison of signal,  $\nu$ -on-e background, and other background events for the reconstructed vertex. No cuts were applied to make these plots. All the previous cuts were applied, including the cut on the shower energy. No single particle or event ID cuts were applied yet though. Gold lines show the cut values that create the fiducial volume.

## 1.5 Energy resolution and binning

**TO DO:** Add the energy resolution and binning plots The electron energy and angle distributions and resolutions. Are we going to fit in E, Th, or ETh2? Is there something else?

Show plots of Reco V True for both energy and angle. (Should I show it with or without the energy cut?). Also show the resolution plots.

Table 1.5: Event selection cutflow table

<b>Selection</b>	<b><math>\nu</math> Mag. Moment signal</b>			<b><math>\nu</math>-on-e background</b>			<b>Other background</b>		
	$N_{sig}$	$\epsilon^{N-1}$	$\epsilon$ (%)	$N_{IBkg}$	$\epsilon^{N-1}$	$\epsilon$ (%)	$N_{Bkg}$	$\epsilon^{N-1}$	$\epsilon$ (%)
<b>No Cut</b>	269.77	100	100	$3.43 \times 10^3$	100	100	$2.96 \times 10^8$	100	100
<b>Vtx Is Valid</b>	180.58	66.94	66.94	$3.33 \times 10^3$	96.94	96.94	$2.34 \times 10^8$	79.09	79.09
<b>N Prongs</b>	174.69	96.74	64.76	$3.23 \times 10^3$	96.99	94.02	$8.66 \times 10^7$	37.00	29.27
<b>Png Length</b>	174.67	99.99	64.75	$3.22 \times 10^3$	99.64	93.68	$7.67 \times 10^7$	88.56	25.92
<b>N Planes</b>	174.67	100	64.75	$3.22 \times 10^3$	99.98	93.67	$7.67 \times 10^7$	99.98	25.92
<b>N Cells</b>	174.67	100	64.75	$3.22 \times 10^3$	99.98	93.65	$7.42 \times 10^7$	96.78	25.08
<b>Closest Slc</b>	169.82	97.22	62.95	$3.14 \times 10^3$	97.54	91.35	$6.95 \times 10^7$	93.68	23.49
<b>Fiducial</b>	167.72	98.76	62.17	$3.09 \times 10^3$	98.41	89.89	$3.59 \times 10^7$	51.71	12.15
<b>Cont.</b>	159.37	95.02	59.08	$2.48 \times 10^3$	80.43	72.30	$1.38 \times 10^7$	38.35	4.66
<b>ShwE Frac.</b>	150.37	94.35	55.74	$2.42 \times 10^3$	97.59	70.56	$8.82 \times 10^6$	63.97	2.98
<b>Vtx E</b>	142.29	94.63	52.74	$2.18 \times 10^3$	90.16	63.62	$4.15 \times 10^6$	47.07	1.40
<b>Shw Gap</b>	137.96	96.96	51.14	$2.09 \times 10^3$	95.58	60.80	$3.25 \times 10^6$	78.34	1.10
<b>Shw E</b>	37.13	26.92	13.76	$1.36 \times 10^3$	65.10	39.58	$6.25 \times 10^5$	19.21	0.21
<b>Nuoneid</b>	29.48	79.39	10.93	940.21	69.18	27.38	$2.42 \times 10^4$	3.88	$8.19 \times 10^{-3}$
<b>Epi0id</b>	22.51	76.35	8.34	749.93	79.76	21.84	$1.47 \times 10^4$	60.75	$4.97 \times 10^{-3}$
<b><math>E\theta^2</math></b>	19.74	87.73	7.32	675.02	90.01	19.66	84.15	0.57	$2.84 \times 10^{-5}$
<b><math>E\theta^2</math> (sb)</b>	2.74	-	1.01	74.30	-	2.16	$1.01 \times 10^3$	-	$3.43 \times 10^{-4}$
<b>No ShwE</b>	37.62	-	13.94	782.67	-	22.79	238.79	-	8.07E-05

## **1.6 Systematic uncertainties**

## **1.7 Fitting and hypothesis testing, parameter estimation**

## **1.8 Results**

## **1.9 Discussion**

## **1.10 Conclusion**

Figure 1.16: Event selection cutflow table for background components

Selection	$N$	$\nu_e \text{CC}$	$\text{MEC}$	$\epsilon_{N-1}$	$\epsilon$ (%)	$N$	$\nu_e \text{CC}$	$\text{Other}$	$\epsilon_{N-1}$	$\epsilon$ (%)	$N$	$\nu_\mu \text{CC}$	$\epsilon_{N-1}$	$\epsilon$ (%)	$N$	$\text{NC}$	$\epsilon_{N-1}$	$\epsilon$ (%)	<b>Other</b>	$\epsilon^{N-1}$	$\epsilon$ (%)
<b>No Cut</b>	$3.50 \times 10^4$	100	$3.23 \times 10^6$	100	100	$2.24 \times 10^8$	100	100	$3.40 \times 10^7$	100	100	$3.49 \times 10^7$	$100$	100	$6.53 \times 10^6$	$18.70$	$18.70$				
<b>Vtx Is Valid</b>	$3.27 \times 10^4$	93.58	93.58	$2.62 \times 10^6$	81.14	81.14	$1.99 \times 10^8$	$89.02$	$89.02$	$2.57 \times 10^7$	75.55	75.55	$58.57$	44.25	$2.65 \times 10^6$	40.51	7.58				
<b>N Prongs</b>	$2.74 \times 10^4$	83.76	78.39	$1.39 \times 10^6$	53.05	43.05	$6.75 \times 10^7$	33.89	30.17	$1.51 \times 10^7$	$99.07$	$99.07$	$43.84$	$2.64 \times 10^6$	$99.87$	7.57					
<b>Prg Length</b>	$2.73 \times 10^4$	99.79	78.22	$1.37 \times 10^6$	98.53	42.42	$5.77 \times 10^7$	85.56	25.81	$1.49 \times 10^7$	100	100	$43.84$	$2.64 \times 10^6$	100	7.57					
<b>N Planes</b>	$2.73 \times 10^4$	99.99	78.22	$1.37 \times 10^6$	99.99	42.41	$5.77 \times 10^7$	99.98	25.81	$1.49 \times 10^7$	$96.34$	$96.34$	$42.24$	$2.64 \times 10^6$	100	7.57					
<b>N Cells</b>	$2.73 \times 10^4$	99.99	78.21	$1.28 \times 10^6$	93.49	39.65	$5.59 \times 10^7$	96.82	24.98	$1.44 \times 10^7$	$94.17$	$94.17$	$39.77$	$1.43 \times 10^6$	$54.22$	4.10					
<b>Closest SIC</b>	$2.73 \times 10^4$	99.79	78.05	$1.21 \times 10^6$	94.25	37.37	$5.33 \times 10^7$	95.40	23.84	$1.35 \times 10^7$	$94.17$	$94.17$	$39.77$	$1.43 \times 10^6$	$54.22$	4.10					
<b>Fiducial</b>	$1.39 \times 10^4$	51.12	39.90	$6.30 \times 10^5$	52.10	19.47	$2.60 \times 10^7$	48.77	11.62	$8.25 \times 10^6$	60.99	60.99	$24.26$	$1.03 \times 10^6$	73.53	3.02					
<b>Cont.</b>	$9.32 \times 10^3$	66.82	26.66	$2.63 \times 10^5$	41.72	8.12	$7.64 \times 10^6$	29.38	3.42	$4.96 \times 10^6$	60.15	60.15	$14.59$	$9.12 \times 10^5$	86.62	2.61					
<b>ShwE Frac.</b>	$9.20 \times 10^3$	98.70	26.32	$1.95 \times 10^5$	74.39	6.04	$4.82 \times 10^6$	63.10	2.15	$2.97 \times 10^6$	59.78	59.78	$8.72$	$8.28 \times 10^5$	90.81	2.37					
<b>Vtx E</b>	$5.92 \times 10^3$	64.33	16.93	$6.05 \times 10^4$	30.96	1.87	$1.97 \times 10^6$	40.79	0.88	$1.36 \times 10^6$	$45.75$	$45.75$	$3.99$	$7.62 \times 10^5$	$92.03$	2.18					
<b>Shw Gap</b>	$5.50 \times 10^3$	92.91	15.73	$4.62 \times 10^4$	76.40	1.43	$1.58 \times 10^6$	80.18	0.70	$1.06 \times 10^6$	$77.78$	$77.78$	$3.10$	$5.69 \times 10^5$	74.61	1.63					
<b>Shw E</b>	$3.62 \times 10^3$	65.81	10.35	$1.12 \times 10^4$	24.15	0.35	$4.38 \times 10^5$	27.80	0.20	$1.71 \times 10^5$	16.15	16.15	$0.50$	$1.28 \times 10^3$	$3.68 \times 10^{-3}$						
<b>Nuoneid</b>	$1.40 \times 10^3$	38.63	4.00	$2.11 \times 10^3$	18.89	0.065	$1.17 \times 10^4$	2.66	$5.21 \times 10^{-3}$	$8.99 \times 10^3$	5.27	5.27	$0.026$	66.43	5.17	$1.90 \times 10^{-4}$					
<b>Epi01d</b>	$1.14 \times 10^3$	81.78	3.27	$1.61 \times 10^3$	76.40	0.050	$7.17 \times 10^3$	61.52	$3.20 \times 10^{-3}$	$4.76 \times 10^3$	52.94	52.94	$0.014$	29.47	44.36	$8.44 \times 10^{-5}$					
<b><math>E\theta^2</math></b>	$15.13$	1.32	0.043	39.00	2.42	$1.21 \times 10^{-3}$	8.62	$3.85 \times 10^{-6}$	20.91	0.44	$6.15 \times 10^{-5}$	0.50	$1.69$	$1.43 \times 10^{-6}$	-						
<b><math>E\theta^2</math> (sb)</b>	386.16	-	1.10	306.55	-	$9.48 \times 10^{-3}$	165.59	-	$7.40 \times 10^{-5}$	149.93	-	$4.41 \times 10^{-4}$	6.24	-	$1.79 \times 10^{-5}$						
<b>No ShwE</b>	15.54	-	0.044	69.61	-	$2.15 \times 10^{-3}$	68.48	-	$3.06 \times 10^{-5}$	75.67	-	$2.22 \times 10^{-4}$	9.49	-	$2.72 \times 10^{-5}$						



# Acronyms

**$\nu$ -on-e** neutrino-on-electron. 10, 11, 13–17, 20

**BSM** Beyond Standard Model. 1, 3, 6

**CC** Charged Current. 10, 16, 21

**LDM** Light Dark Matter. 15, 20

**MEC** Meson Exchange Current. 16

**ND** Near Detector. 6, 14, 15, 20

**NOvA** NuMI Off-axis  $\nu_e$  Appearance (experiment). 5, 10, 12–15, 20

**NP** New Physics. 4

**PMNS** Pontecorvo-Maki-Nakagawa-Sakata. 3–5

**SM** Standard Model. 1–3, 10–15

# Bibliography

- [1] Patrick Huber et al. Snowmass Neutrino Frontier Report. In *Snowmass 2021*, 11 2022.
- [2] Carlo Giunti and Alexander Studenikin. Neutrino electromagnetic interactions: A window to new physics. *Rev. Mod. Phys.*, 87:531–591, Jun 2015. doi:[10.1103/RevModPhys.87.531](https://doi.org/10.1103/RevModPhys.87.531).
- [3] Boris Kayser. Majorana neutrinos and their electromagnetic properties. *Phys. Rev. D*, 26:1662–1670, Oct 1982. doi:[10.1103/PhysRevD.26.1662](https://doi.org/10.1103/PhysRevD.26.1662). URL <https://link.aps.org/doi/10.1103/PhysRevD.26.1662>.
- [4] José F. Nieves. Electromagnetic properties of majorana neutrinos. *Phys. Rev. D*, 26:3152–3158, Dec 1982. doi:[10.1103/PhysRevD.26.3152](https://doi.org/10.1103/PhysRevD.26.3152). URL <https://link.aps.org/doi/10.1103/PhysRevD.26.3152>.
- [5] Carlo Giunti, Julieta Gruszko, Benjamin Jones, Lisa Kaufman, Diana Parno, and Andrea Pocar. Report of the Topical Group on Neutrino Properties for Snowmass 2021. 9 2022.
- [6] Nicole F. Bell, Mikhail Gorchtein, Michael J. Ramsey-Musolf, Petr Vogel, and Peng Wang. Model independent bounds on magnetic moments of Majorana neutrinos. *Phys. Lett. B*, 642:377–383, 2006. doi:[10.1016/j.physletb.2006.09.055](https://doi.org/10.1016/j.physletb.2006.09.055).

## APPENDIX A

# Test Beam Calibration Validation Plots

### A.1 Distributions for Stopping Muons

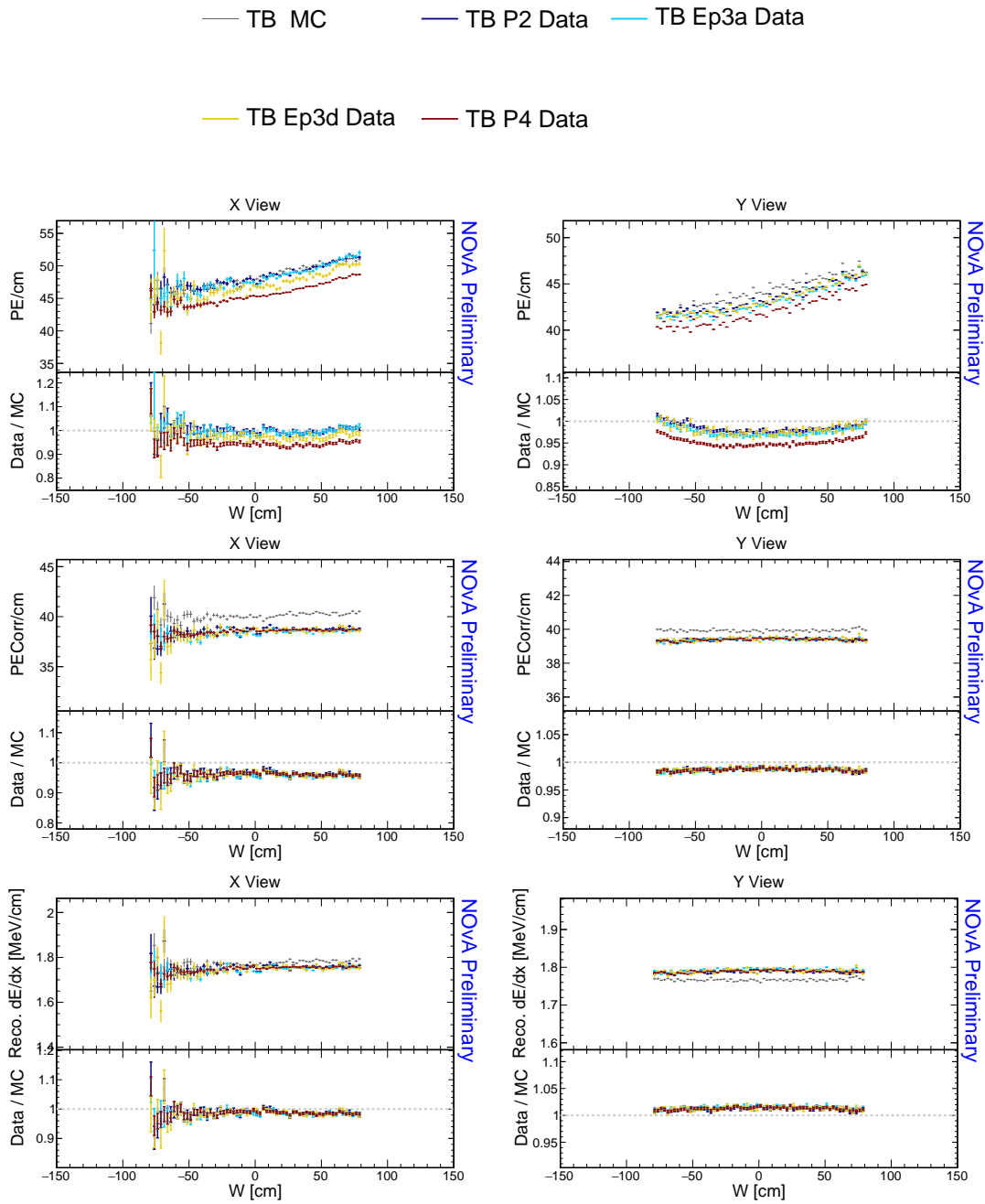


Figure A.1: Distributions of stopping muons within a 1-2 m track window from the end of their tracks across the position within a cell.

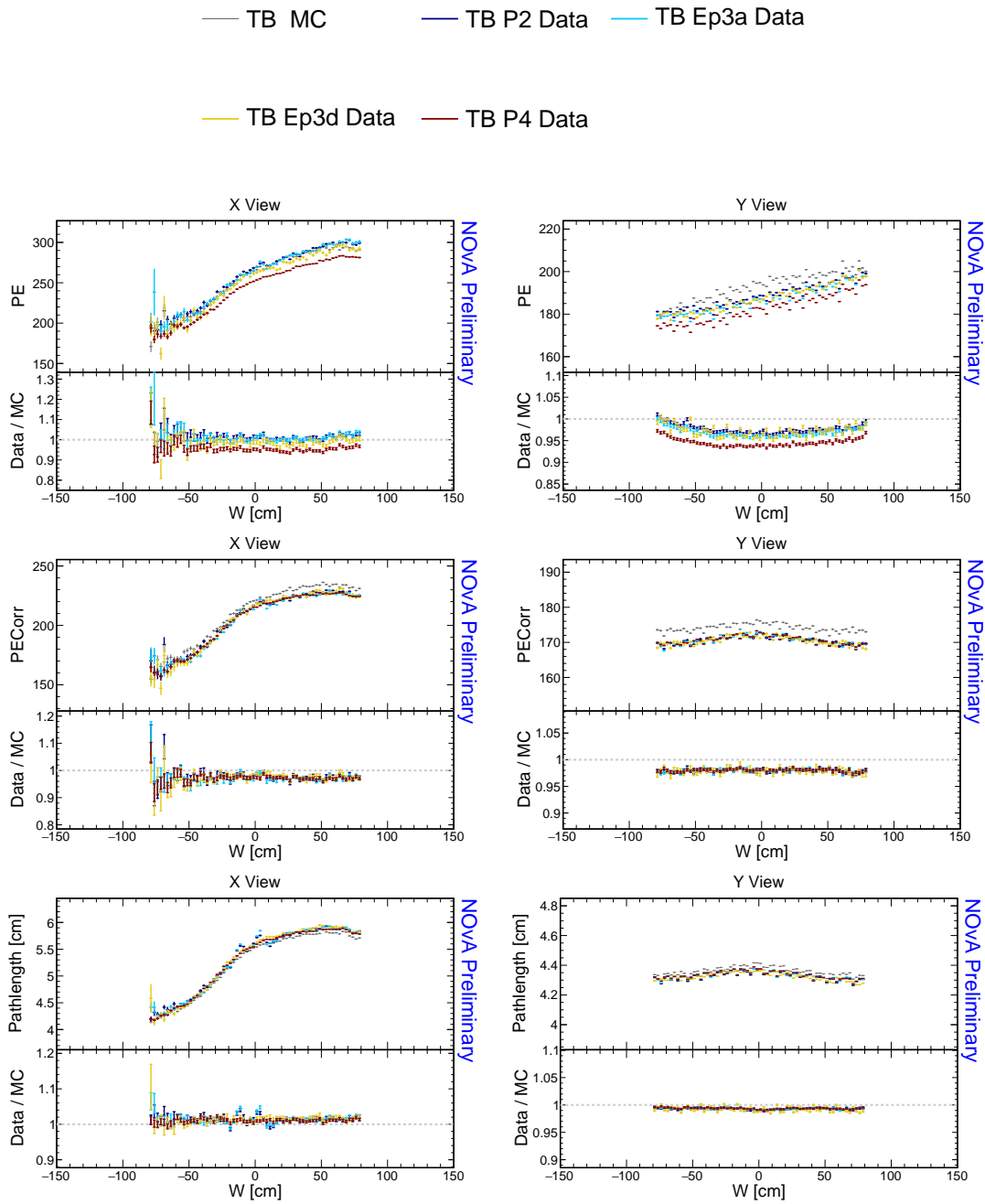


Figure A.2: Distributions of stopping muons within a 1-2 m track window from the end of their tracks across the position within a cell.

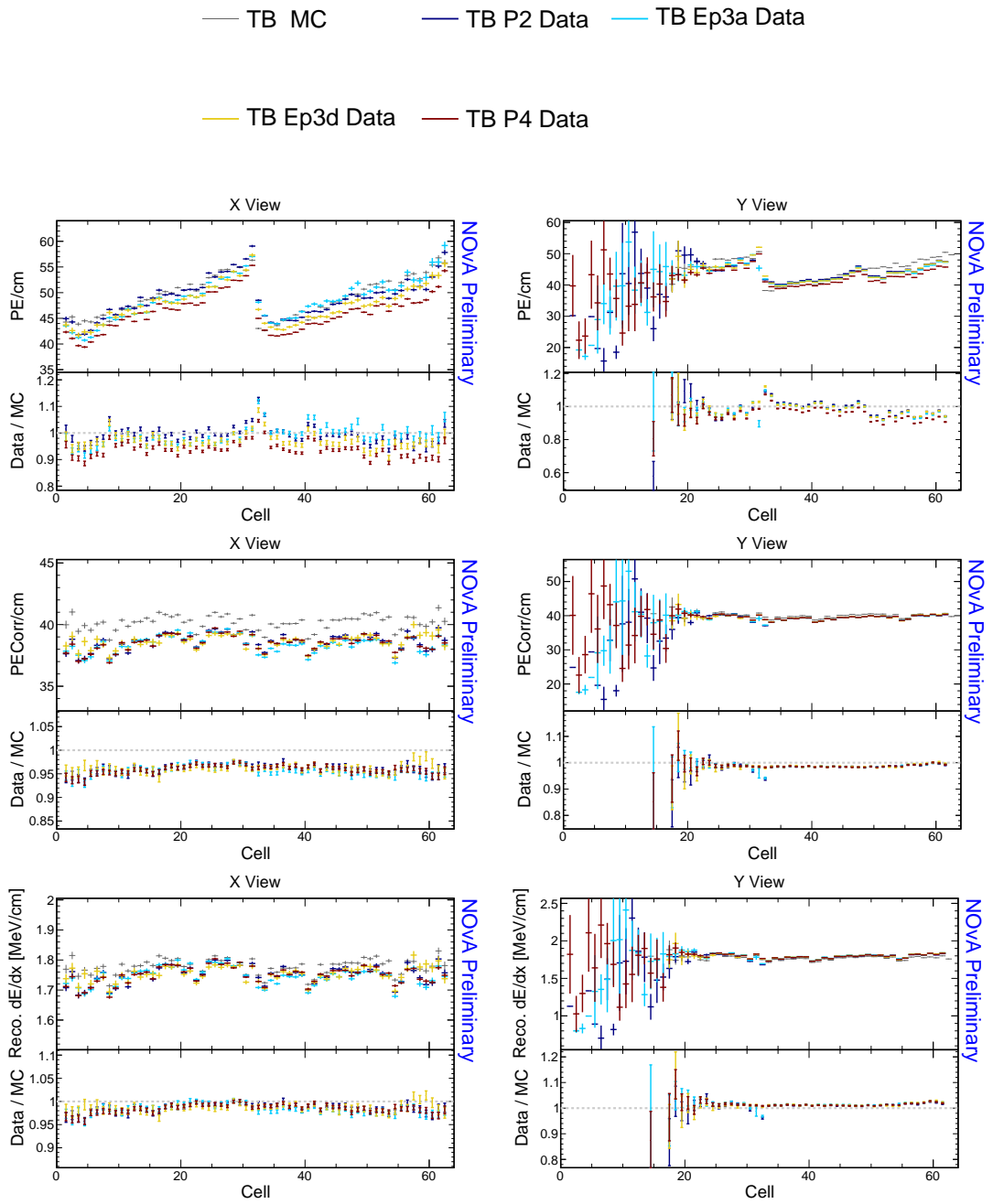


Figure A.3: Distributions of stopping muons within a 1-2 m track window from the end of their tracks across the cells of the detector.

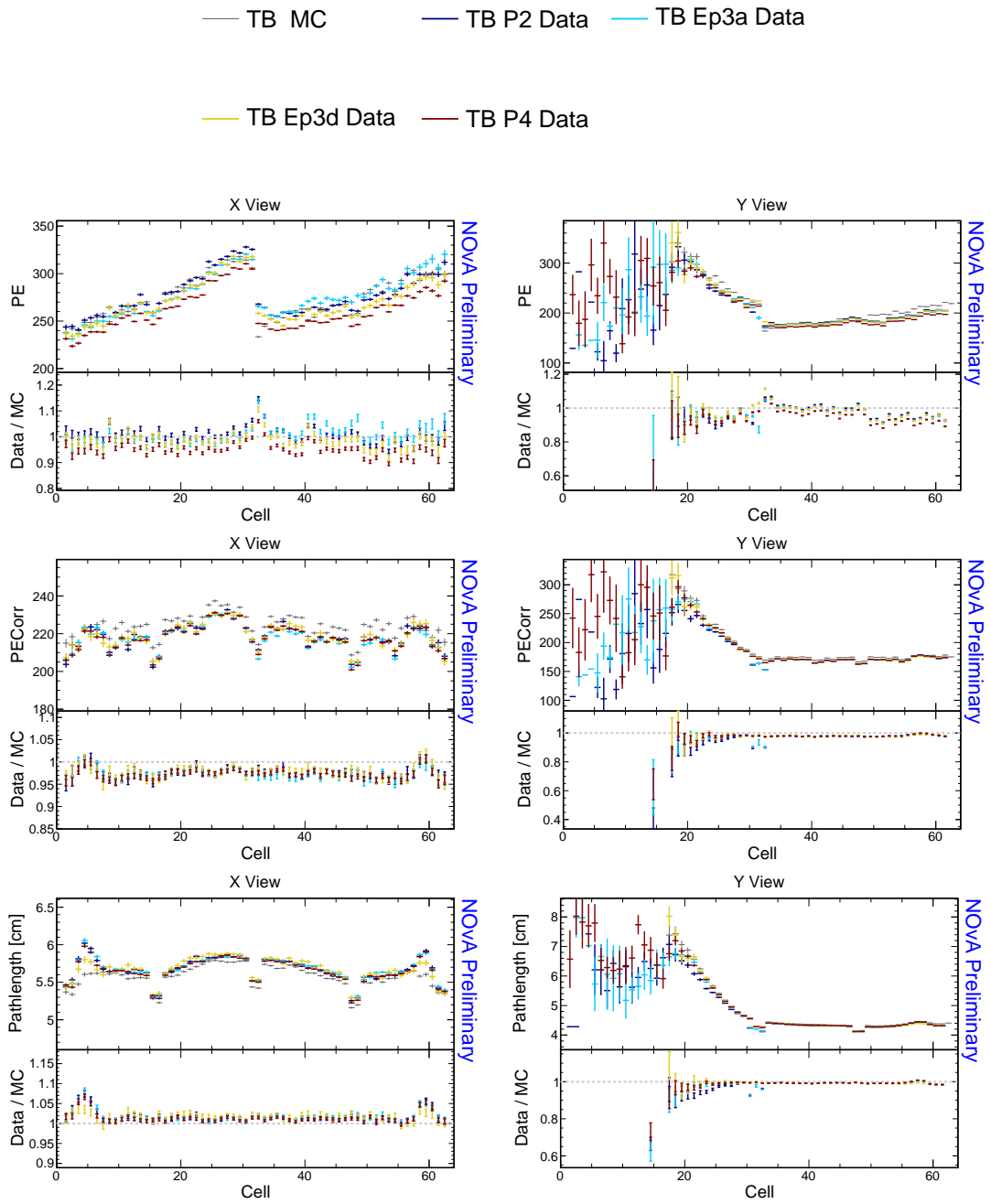


Figure A.4: Distributions of stopping muons within a 1-2 m track window from the end of their tracks across the cells of the detector.

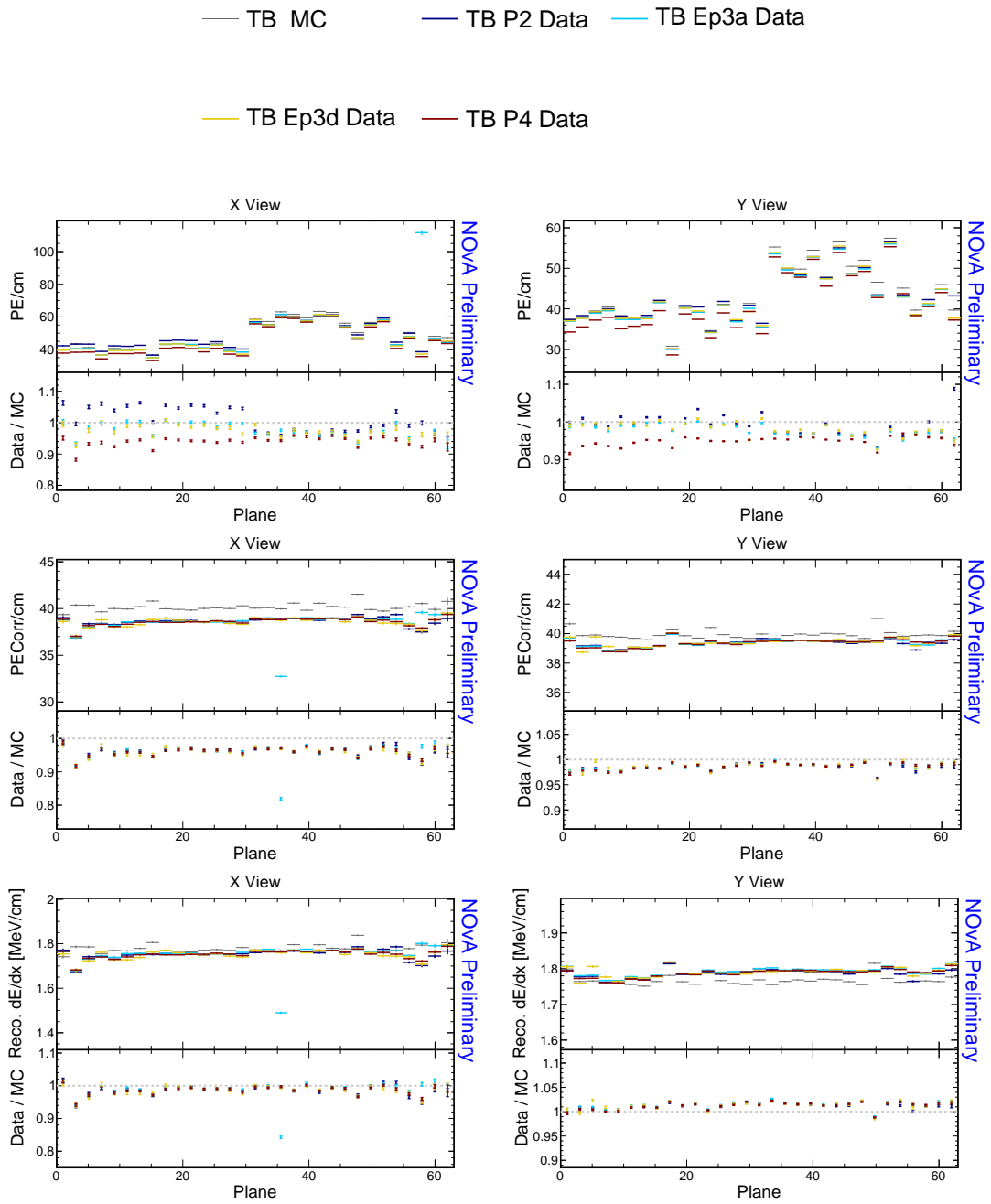


Figure A.5: Distributions of stopping muons within a 1-2 m track window from the end of their tracks across the planes of the detector.

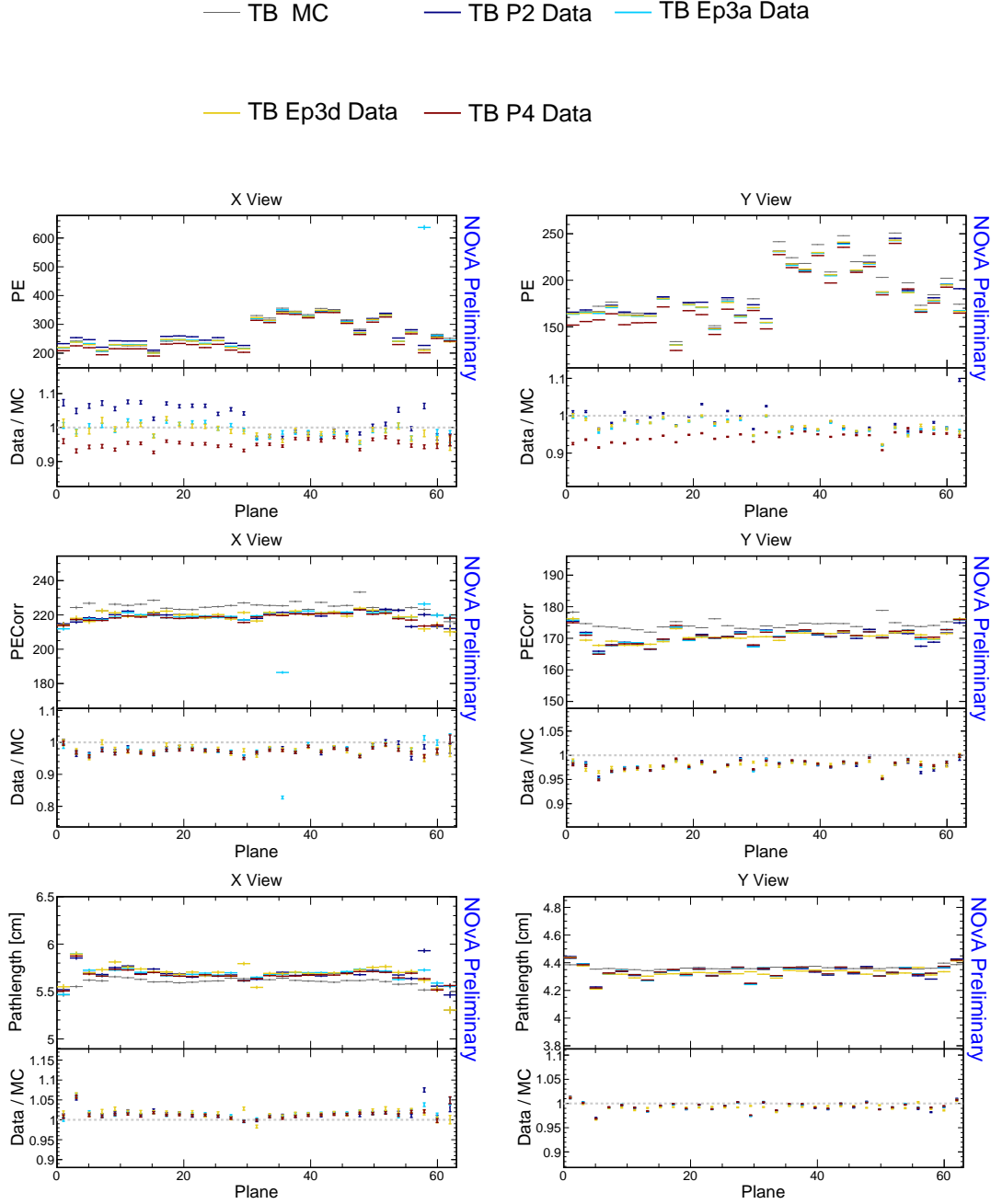


Figure A.6: Distributions of stopping muons within a 1-2 m track window from the end of their tracks across the planes of the detector.

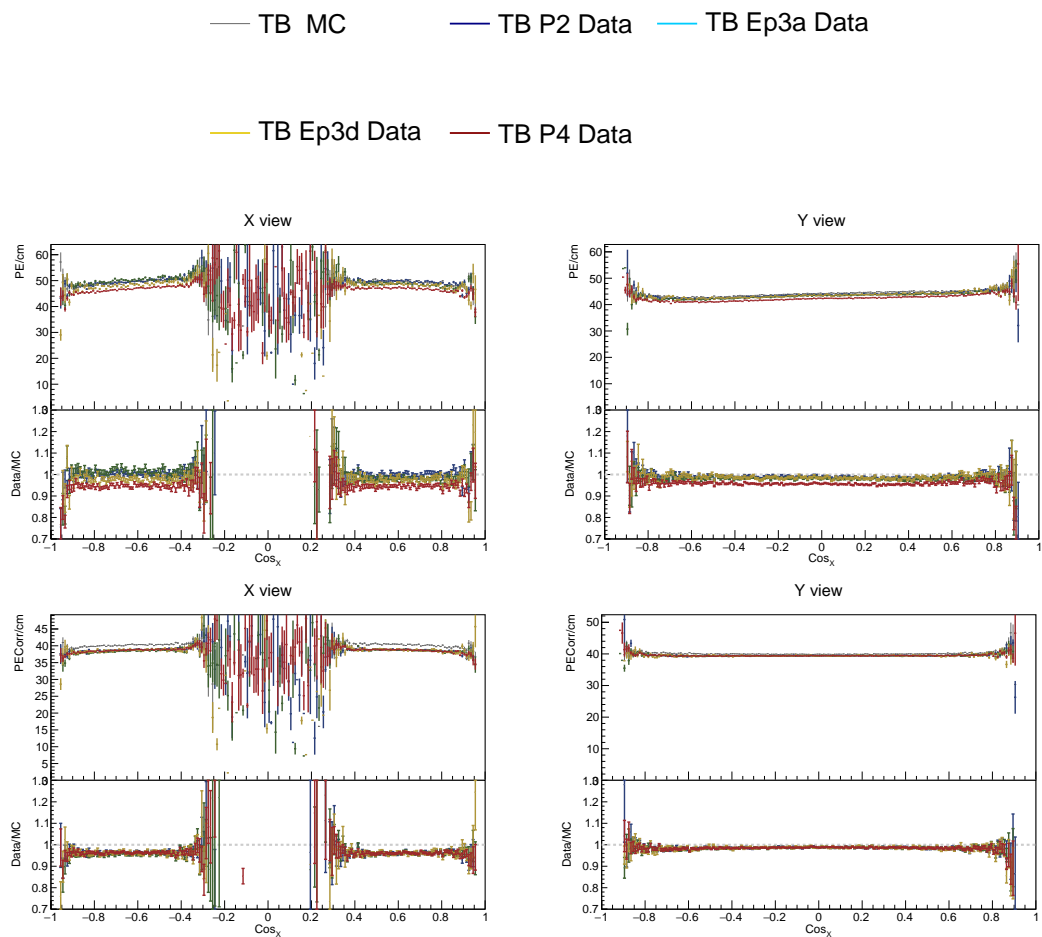


Figure A.7: Distributions of stopping muons within a 1-2 m track window from the end of their tracks across the cosine of the track angle from the X (horizontal) axis.

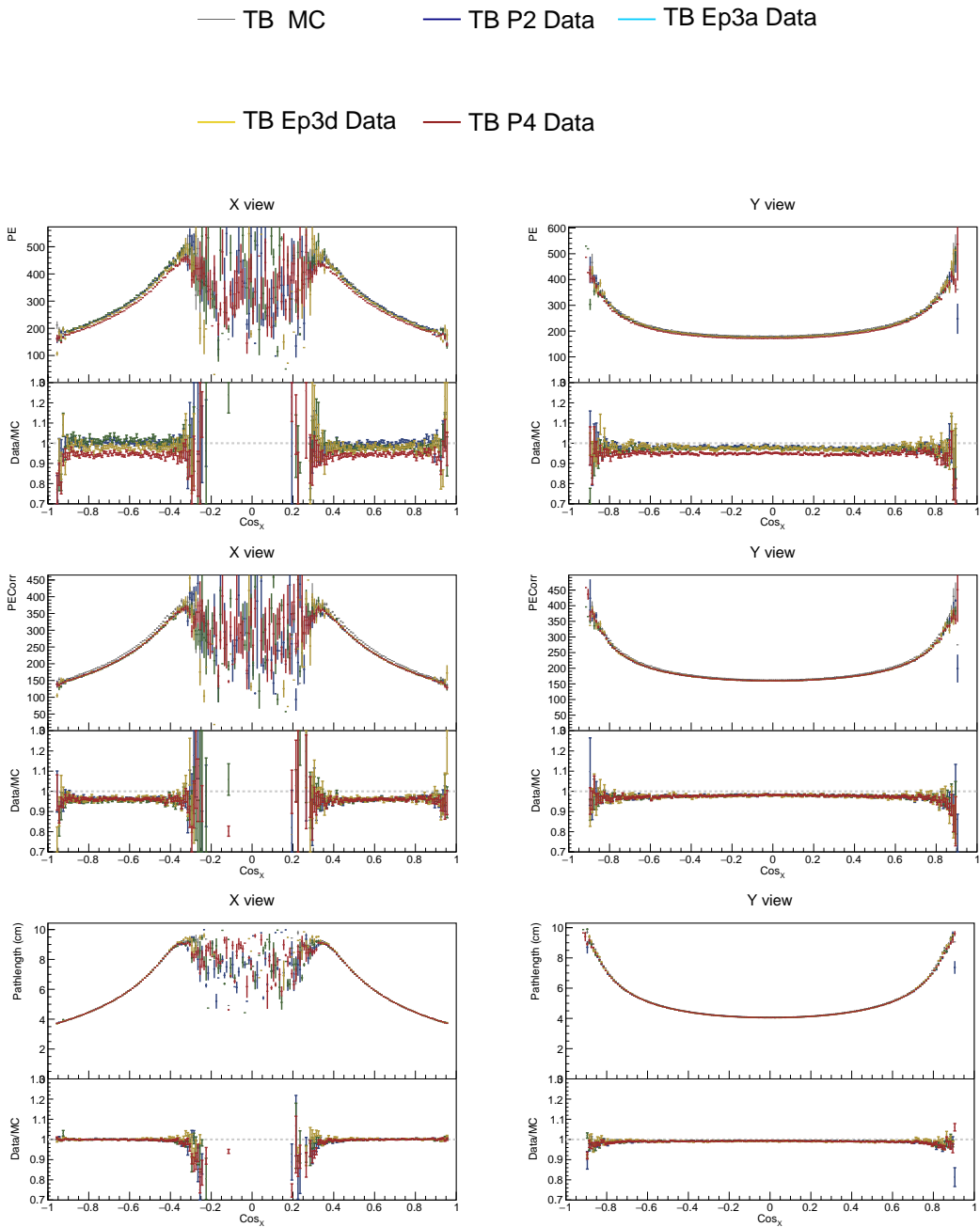


Figure A.8: Distributions of stopping muons within a 1-2 m track window from the end of their tracks across the cosine of the track angle from the X (horizontal) axis.

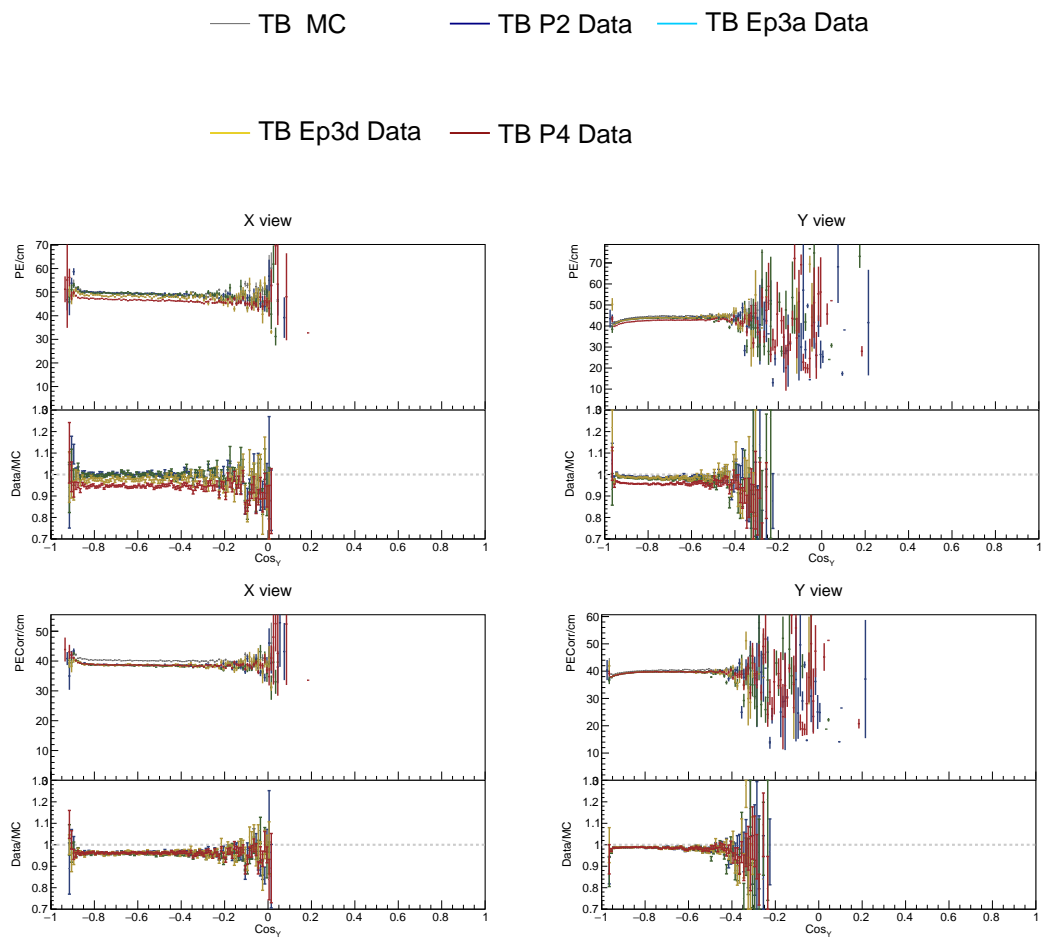


Figure A.9: Distributions of stopping muons within a 1-2 m track window from the end of their tracks across the cosine of the track angle from the Y (vertical) axis.

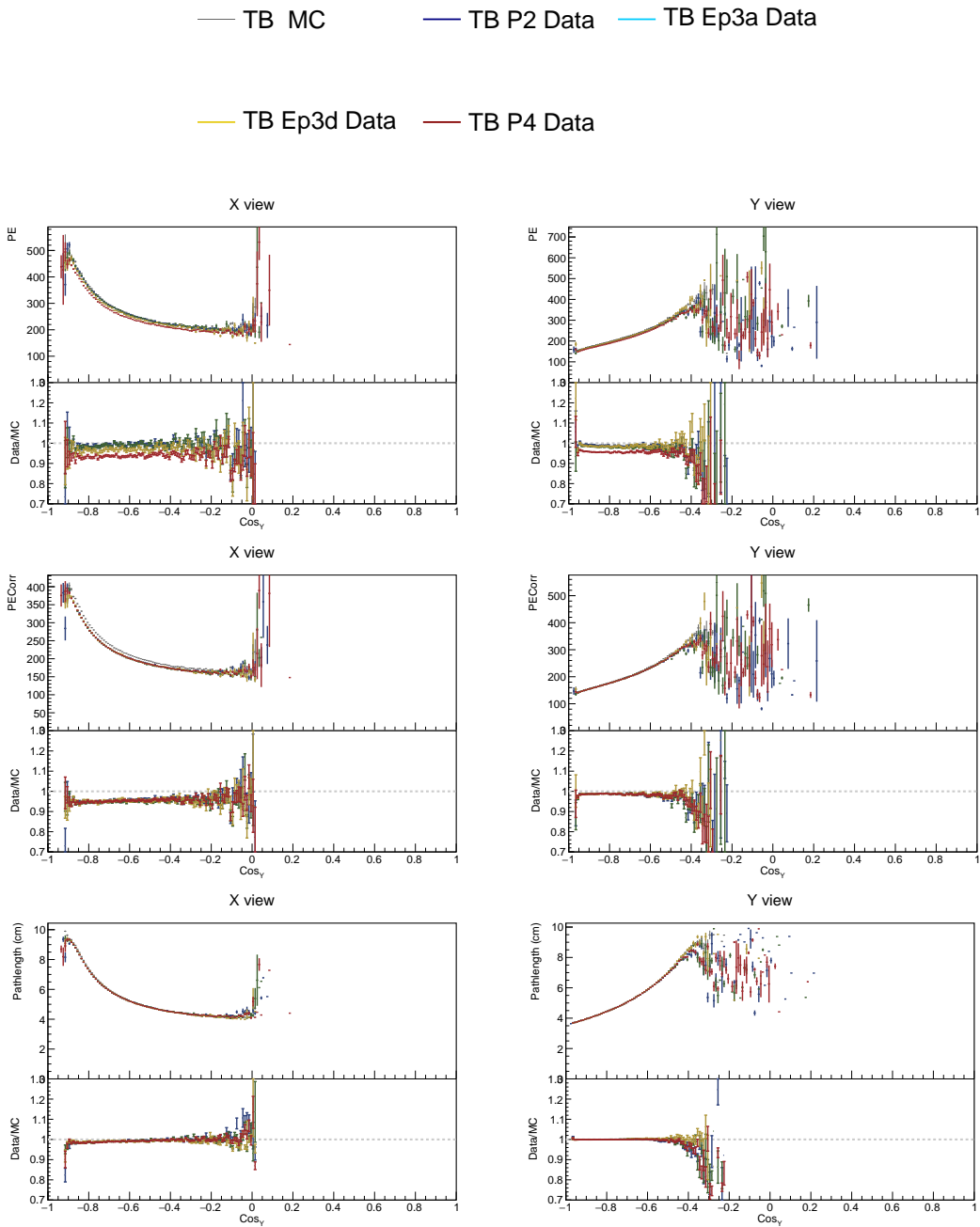


Figure A.10: Distributions of stopping muons within a 1-2 m track window from the end of their tracks across the cosine of the track angle from the Y (vertical) axis.

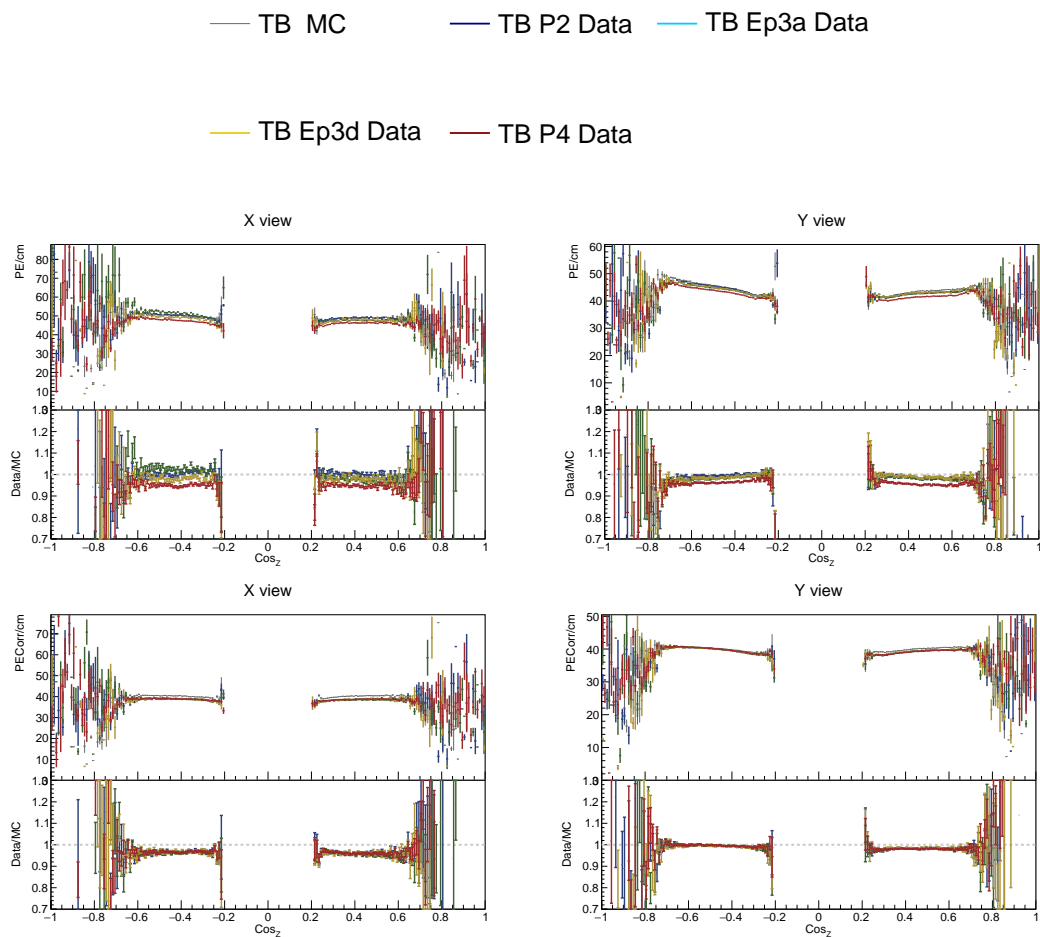


Figure A.11: Distributions of stopping muons within a 1-2 m track window from the end of their tracks across the cosine of the track angle from the Z (beam) axis.

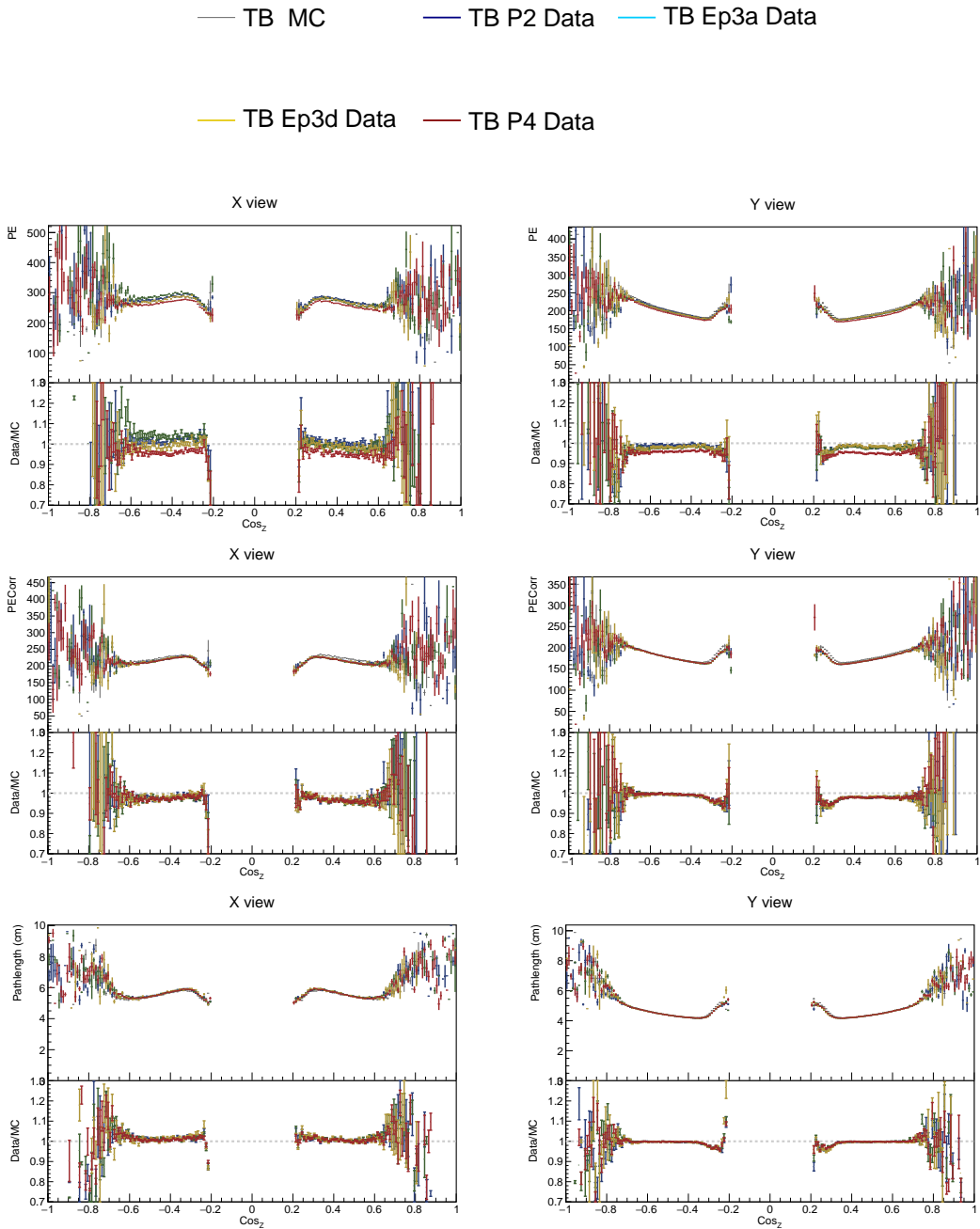


Figure A.12: Distributions of stopping muons within a 1-2 m track window from the end of their tracks across the cosine of the track angle from the Z (beam) axis.

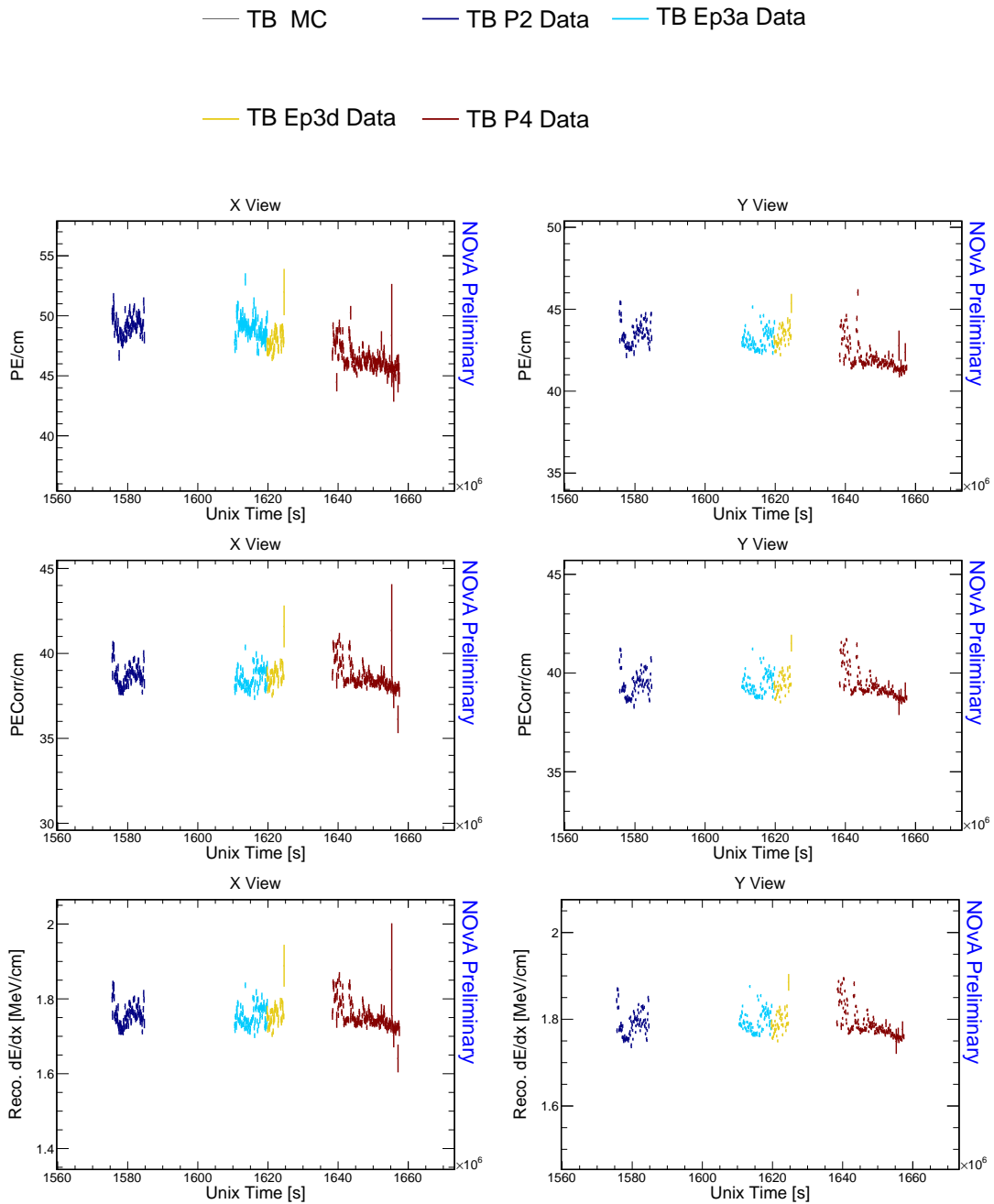


Figure A.13: Distributions of stopping muons within a 1-2 m track window from the end of their tracks across the event UNIX time.

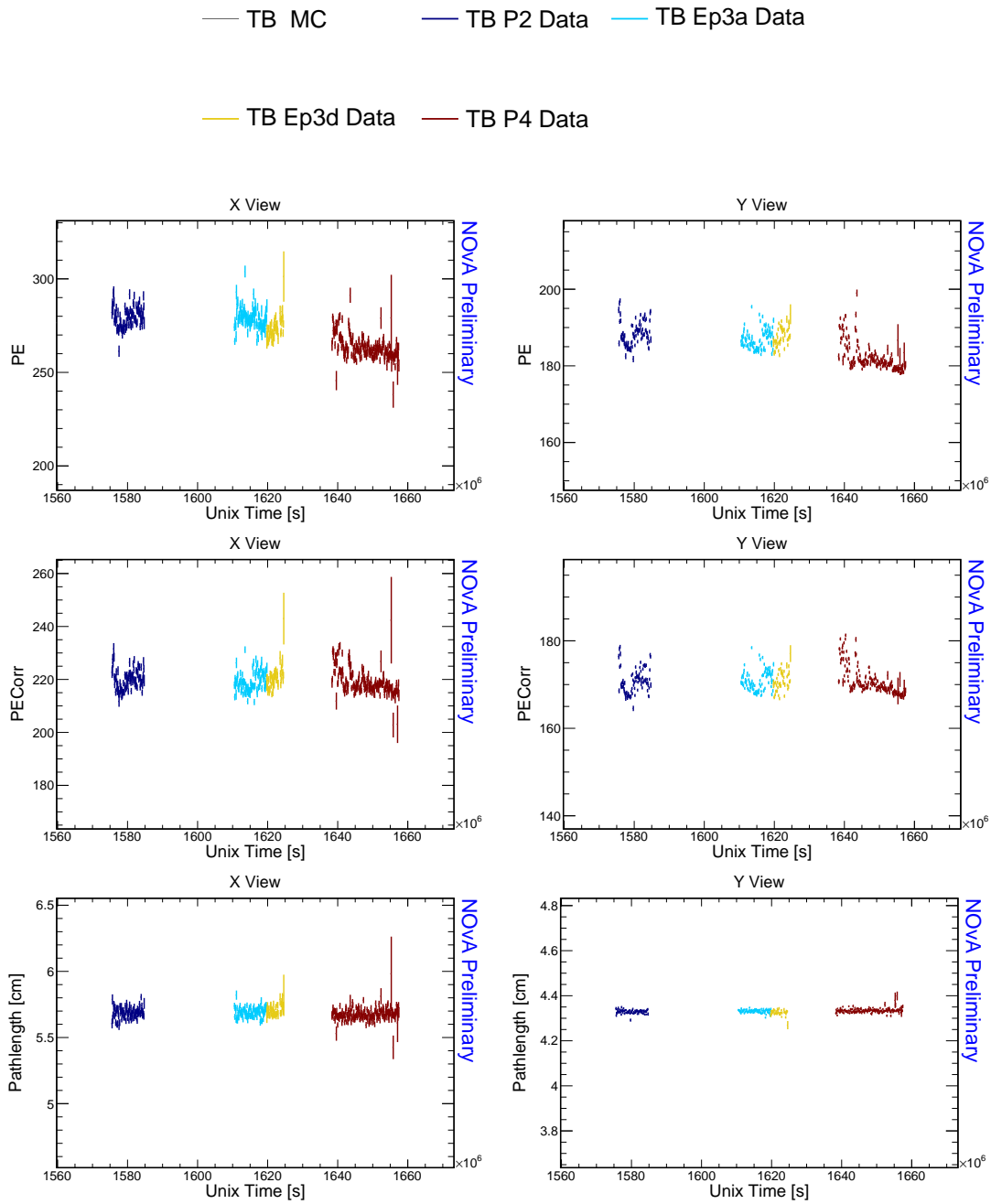


Figure A.14: Distributions of stopping muons within a 1-2 m track window from the end of their tracks across the event UNIX time.

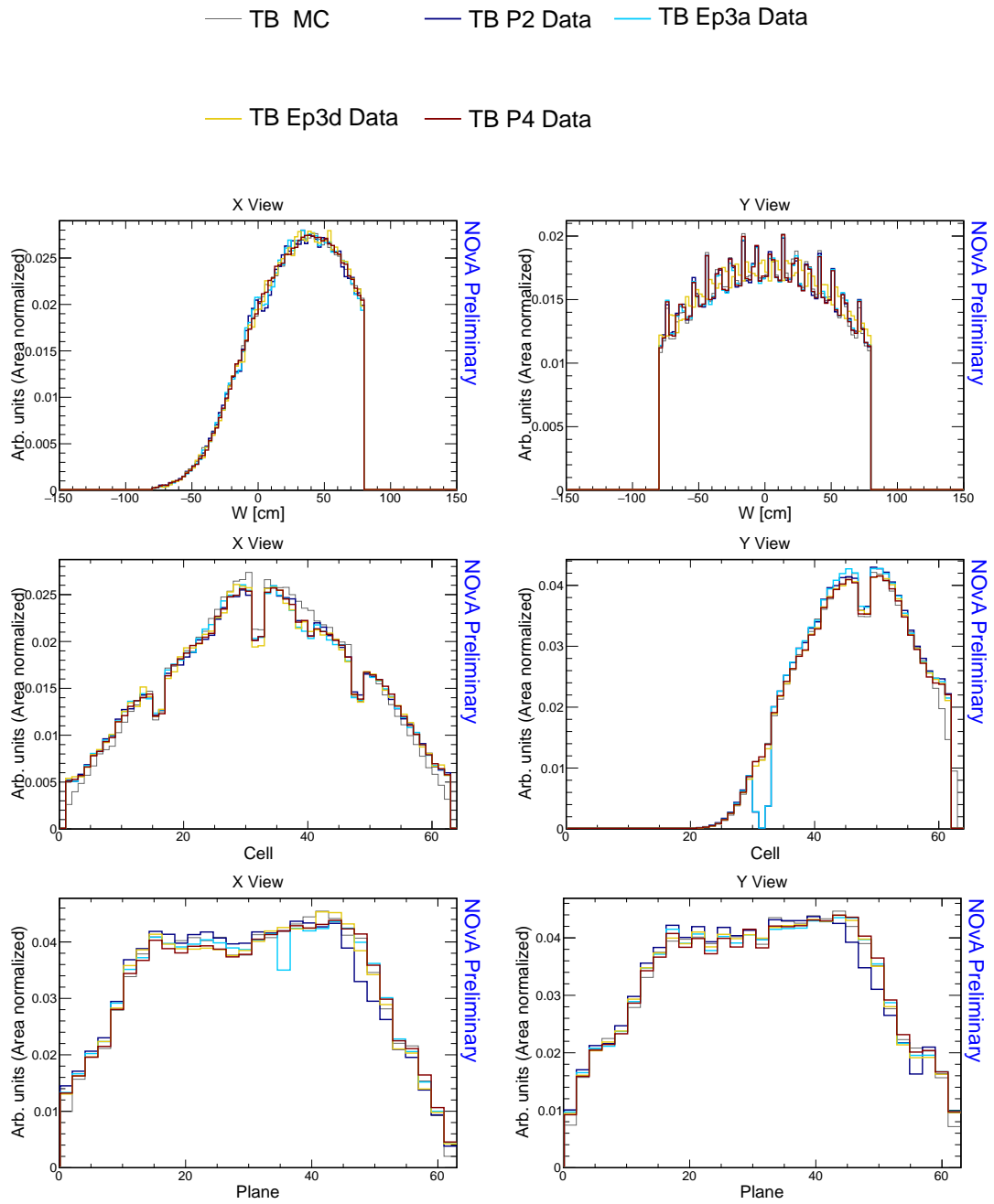


Figure A.15: Distributions of stopping muons within a 1-2 m track window from the end of their tracks.